

Gravitational radiation from collapsing magnetized dust

Hajime Sotani^{1,*}, Shijun Yoshida^{2,†} and Kostas D. Kokkotas^{1‡}

¹*Department of Physics, Aristotle University of Thessaloniki, Thessaloniki 54124, Greece*

²*Science and Engineering, Waseda University, Okubo, Shinjuku, Tokyo 169-8555, Japan*

(Dated: October 13, 2018)

In this article we study the influence of magnetic fields on the axial gravitational waves emitted during the collapse of a homogeneous dust sphere. We found that while the energy emitted depends weakly on the initial matter perturbations it has strong dependence on the strength and the distribution of the magnetic field perturbations. The gravitational wave output of such a collapse can be up to an order of magnitude larger or smaller calling for detailed numerical 3D studies of collapsing magnetized configurations.

PACS numbers: 04.25.Nx, 04.30.Db, 04.40.Dg

I. INTRODUCTION

The direct detection of gravitational waves will be a significant breakthrough both for fundamental physics and astrophysics. With the information collected from gravitational waveforms, one will be able to make validation of general relativity, collection of astronomical data, and examine the nature of matter in supranuclear densities. Among the most important applications of the gravitational wave observations is the asteroseismology in which seismic information for determining stellar structures is obtained by gravitational waveforms [1, 2, 3, 4, 5, 6, 7]. Currently, several ground-based acoustic and laser interferometric detectors for gravitational waves like LIGO, TAMA300, GEO600, and VIRGO are in operation but there is not yet any direct detection of gravitational waves [8]. In addition to the ground-based detectors, there is a project to launch a Laser Interferometric Space Antenna (LISA), which is planned to be launched by the end of next decade and to operate for five years [9].

The nonspherical stellar collapse is one of the potential sources of gravitational waves both for the ground-based and for space detectors. The ground-based interferometers target the formation of stellar mass black holes or neutron stars because they are most sensitive to gravitational wave frequencies in the range 10 – 1000 Hz. Space detectors with sensitivities ranging from 10^{-4} up to 10^{-1} Hz might detect signals from the creation of supermassive black-holes [10, 11, 12, 13, 14, 15]. There are two approaches to calculate the energy radiated away as gravitational radiation during stellar collapse; the first is via direct numerical integration of the exact Einstein and matter equations, which form a coupled nonlinear system of partial differential equations, and the second is by making use of the linear perturbation analysis. During the last decade numerical relativity made remarkable advances and many complicated matter and spacetime configurations can be treated with high degree of confidence [16, 17, 18, 19, 20, 21].

In spite of the recent great progress in numerical relativity, the accurate extraction of gravitational waveforms has been proved a quite difficult task. The reason is that the weak gravitational waves emitted during the stellar collapse sometimes have amplitudes similar to those of unphysical noises due to gauge modes and/or to numerical errors. Linear perturbation theory is extremely efficient for such processes since the nonradial perturbations which are responsible for the emission of the weak gravitational waves are separated from the nonradiative symmetric background. For example, for spherically symmetric backgrounds the physical quantities described by the perturbations can be expanded in terms of tensor spherical harmonics and this separation of variables simplifies considerably the study of the problem. Actually, the master equations for the perturbations are reduced to simple set of coupled linear partial differential equations, which can be evolved with extremely high accuracy. On the other hand via this procedure one might miss certain nonlinear phenomena that take place at the very last stages of collapse.

Linear perturbation analysis has been used in calculations of the gravitational wave emission from the stellar collapse to a black hole [22, 23, 24, 25]. Cunningham, Price, and Moncrief derived the perturbation equations on the Oppenheimer-Snyder solution, which describes collapse of homogeneous dust [26] and calculated gravitational radiation emitted during the collapse to a black hole [22]. By using the gauge invariant perturbation formalism on the spherically symmetric spacetime formulated by Gerlach and Sengupta [27], Seidel and co-workers [23] investigated the

*Electronic address: sotani@gravity.phys.waseda.ac.jp

†Electronic address: yoshida@heap.phys.waseda.ac.jp

‡Electronic address: kokkotas@astro.auth.gr

gravitational waves from the stellar collapse in which a neutron star is born. The gravitational waves from collapse of an inhomogeneous dust, which can be described by nonradial perturbations of the Lemaître-Tolman-Bondi solution [28], are computed by Iguchi, Nakao, and Harada [24]. Harada, Iguchi, and Shibata [25] calculated the axial parity gravitational waves emitted from collapse of a supermassive star to a black hole by employing the covariant gauge-invariant formalism for nonradial perturbations on spherically symmetric spacetime and the coordinate-independent matching conditions at stellar surface, devised by Gundlach and Martín-García [29].

Although, as mentioned above, there have been many investigations of gravitational radiation from stellar collapse with the linear perturbation analysis, effects of magnetic fields on the gravitational radiation have not been taken into account. While Cunningham *et al.* dealt with electromagnetic perturbations of the Oppenheimer-Snyder solution [22], they omitted the conduction of the fluid. In other words, Cunningham *et al.* did not consider the direct coupling between fluid and magnetic field. However, it has been recently realized the importance of effects of magnetic fields on the evolution of compact objects again due to the advent of high-performance instruments like satellite-borne detectors. One of the most impressive examples is the discovery of magnetars, which are neutron stars whose strength of magnetic fields is estimated about 10^{15} G. The magnetar model, in which observed activities are powered by decay of the strong magnetic fields of magnetars, successfully explains activity of soft gamma-ray repeaters (SGRs). All the four of the known SGRs have rotation periods of $\sim 5 - 8$ s, and the three of them have large period derivatives of $\sim 10^{-10}$ s s^{-1} , which infer the existence of magnetic fields of $B \approx (5-8) \times 10^{14}$ G [30]. Since there is an ultra strong magnetic field in some neutron stars, which will be born by stellar collapse, it is natural to take into account its effect on stellar collapse. Even if the initial magnetic field is weak, it is conceivable that the magnetic fields of the collapsing object are, due to the magnetic flux conservation, amplified during the collapse and will most probably affect the gravitational waves emitted.

Another example for showing the importance of magnetic fields in the evolution of compact objects is related to gamma-ray bursts (GRBs). The short-duration GRBs could result from hypergiant flares of magnetars associated with the SGRs [31] or magnetized hypermassive neutron star collapse [32]. For long-duration GRBs, strong magnetic fields provide the excitation energy on the required time scale and drive collimated GRB outflows in the form of relativistic jets [33]. Additionally, the so-called hypermassive neutron star, which can be formed after the merger of binary neutron stars and can be in an equilibrium state due to differential rotation, could lead to delayed collapse by the magnetic braking and viscosity, even if the initial magnetic field and the viscosity are very weak [34]. Notice that even if they are weak initially, the magnetic fields can be amplified to the required strength by the winding-up of weak magnetic field due to differential rotation [35, 36].

All the examples mentioned above indeed suggest that magnetic fields play an important role in the stellar collapse. In this paper, we therefore consider gravitational radiation from collapse of weakly magnetized dust spheres to explore the effects of magnetic fields on the gravitational waves from the stellar collapse to a black hole. For the sake of simplicity, we consider, as the background spacetime, the Oppenheimer-Snyder solution, which describes homogeneous dust collapse. The weak magnetic fields of the dust spheres are treated as small perturbations around the Oppenheimer-Snyder solution. We therefore regard both the gravitational waves and the magnetic fields as perturbations on the Oppenheimer-Snyder solution in this study. Thus we introduced, a dimensionless quantity related to the amplitude of gravitational perturbations, $\epsilon \sim |\delta g_{\mu\nu}|$, and another one for the strength of the magnetic field, $\eta \sim |B/(GM^2R^{-4})^{1/2}|$. Here $\delta g_{\mu\nu}$ stands for the metric perturbation and B for the magnetic field strength while M and R denote the mass and radius of the star. Note that in this work we assume that the Lagrangian displacement of the fluid ξ^μ satisfies the condition $|\xi^\mu|/R \sim \epsilon$. It should be emphasized that a perturbative treatment of the magnetic fields is good enough to describe the strong magnetic fields met in magnetars because dynamics of the stellar collapse is basically governed by gravity. In other words, the ratio of the magnetic energy \mathcal{E}_M to the gravitational energy \mathcal{E}_G is sufficiently small even for magnetars, i.e. a typical value of $\mathcal{E}_M/\mathcal{E}_G$ for magnetars is approximated by $\mathcal{E}_M/\mathcal{E}_G \approx B^2/(GM^2R^{-4}) \approx 10^{-4} \times (B/10^{16}[\text{G}])$. As for gravitational perturbations, this paper focus on the axial parity perturbations as the first step. The axial parity gravitational waves are treated with the covariant gauge-invariant formalism. We further assume that the two expansion parameters, ϵ and η , satisfy $\epsilon \sim \eta^2$. In other words, we consider the gravitational radiation directly driven by the magnetic field of the dust sphere.

This paper is organized as follows. In §II we make a short introduction on the orders of the various perturbative quantities that we use, then we briefly describe the gauge-invariant perturbation theory, and finally we show the form of the basic equations describing the magnetic fields. Next, in §III, we describe the formulation for the magnetized homogeneous dust collapse including an analytic description of the background spacetime, the magnetic fields, the axial parity perturbation equations and the junction conditions at stellar surface. In §IV, we describe the details of numerical procedures employed in this study, while the code test are presented in §V. The results related to the efficiency of the collapsing magnetized homogeneous dust spheres in gravitational wave emission are shown in §VI. The final section, §VII, is devoted to discussion and conclusions. In this paper, we adopt the unit of $c = G = 1$, where c and G denote the speed of light and the gravitational constant, respectively, and the metric signature is $(-, +, +, +)$.

II. PERTURBATION THEORY PRIMER

A. Ordering of Perturbations

Since the energy of the magnetic field is much smaller than that of the gravity even for magnetars, as mentioned in the previous section, it is reasonable to treat the electromagnetic field in the dust sphere as small perturbations. The perturbed metric, $\tilde{g}_{\mu\nu}$, the perturbed four-velocity of the fluid, \tilde{u}^μ , and the perturbed electromagnetic tensor, $\tilde{F}_{\mu\nu}$, can be expanded as:

$$\tilde{g}_{\mu\nu} = g_{\mu\nu} + \delta g_{\mu\nu} + \mathcal{O}(\epsilon^2), \quad (1)$$

$$\tilde{u}^\mu = u^\mu + \delta u^\mu + \mathcal{O}(\epsilon^2), \quad (2)$$

$$\tilde{F}_{\mu\nu} = F_{\mu\nu} + \delta F_{\mu\nu} + \mathcal{O}(\eta^2), \quad (3)$$

where $g_{\mu\nu}$ is the background metric tensor, u^μ , the four-velocity of the fluid and $F_{\mu\nu}$ the electromagnetic tensor. Both $g_{\mu\nu}$ and u^μ are defined as solutions of a collapsing spherical dust sphere in the absence of any electromagnetic field. For convenience we introduced two small dimensionless parameters related to strength of the magnetic field and to amplitude of the gravitational waves, i.e., $\eta \sim |B/(GM^2R^{-4})^{1/2}|$ and $\epsilon \sim |\delta g_{\mu\nu}|$. Moreover, we assume that the Lagrangian displacement is small i.e. $|\xi^\mu|/R \sim \epsilon$. Finally, we need to mention that in this study, we consider an infinitely conductive fluid, i.e. we make use of the so called ideal magnetohydrodynamic approximation. Thus, the master equations for describing the magnetic field are given by the perfect conductivity condition, $\tilde{F}_{\mu\nu}\tilde{u}^\nu = 0$, and the Maxwell equation $\tilde{F}_{\mu\nu,\alpha} + \tilde{F}_{\nu\alpha,\mu} + \tilde{F}_{\alpha\mu,\nu} = 0$. The first order (η^1) form of the above two conditions will be written as:

$$\delta F_{\mu\nu}u^\nu = 0, \quad (4)$$

$$\delta F_{\mu\nu,\alpha} + \delta F_{\nu\alpha,\mu} + \delta F_{\alpha\mu,\nu} = 0, \quad (5)$$

which determine the magnetic field corrections to the spherical dust sphere. Up to this order of approximation, the variations induced by the presence of the magnetic field do not affect the spherical symmetry of the system, since the Lorentz force which induces deformations in the geometry is of second order (η^2).

In a similar fashion, both the Einstein tensor and the energy-momentum tensor can be expanded in powers of ϵ and η as

$$\tilde{G}_{\mu\nu} = G_{\mu\nu} + \delta G_{\mu\nu} + \mathcal{O}(\epsilon^2), \quad (6)$$

$$\tilde{T}_{\mu\nu}^{(M)} = T_{\mu\nu}^{(M)} + \delta T_{\mu\nu}^{(M)} + \mathcal{O}(\epsilon^2), \quad (7)$$

$$\tilde{T}_{\mu\nu}^{(EM)} = \delta T_{\mu\nu}^{(EM)} + \mathcal{O}(\epsilon\eta^2), \quad (8)$$

where $T_{\mu\nu}^{(M)}$ and $T_{\mu\nu}^{(EM)}$ stand for the energy-momentum tensors for the fluid and for the electromagnetic fields, respectively, while $\delta T_{\mu\nu}^{(EM)}$ is of second order in η . The Einstein equations of order $\eta^0\epsilon^0$ are the evolution equations describing the unperturbed spherical dust collapse. Here we focus in the study of the influence of magnetic field on the efficiency of gravitational wave emission during the collapse, and thus we consider only those terms of the approximation that will be significant in this study. That is we omit terms such as $\eta^0\epsilon^1$ and we further assume that $\epsilon \sim \eta^2$. In this order of approximation, the Einstein equations of order ϵ are reduced to the following form

$$\delta G_{\mu\nu} = 8\pi\{\delta T_{\mu\nu}^{(M)} + \delta T_{\mu\nu}^{(EM)}\} + \mathcal{O}(\epsilon^2) = 8\pi\delta T_{\mu\nu} + \mathcal{O}(\epsilon^2), \quad (9)$$

which describes gravitational perturbations driven both by the magnetic field and the fluid motions of the collapsing dust sphere.

B. Gauge-Invariant Perturbation Theory

The gauge-invariant perturbation theory for spherically symmetric background spacetime has been formulated by Gerlach and Sengupta [27] while its covariant formulations has been developed by Gundlach and Martín-García [29]. Here we only briefly describe this formalism for special case of axial parity perturbations.

1. Background Spacetime

A spherically symmetric four dimensional spacetime \mathcal{M} can be decomposed as a product of the form $\mathcal{M} = \mathcal{M}^2 \times \mathcal{S}^2$, where \mathcal{M}^2 is a 2-dimensional (1+1) reduced spacetime and \mathcal{S}^2 a 2-dimensional spheres. In other words, the metric $g_{\mu\nu}$ and the stress-energy tensor $T_{\mu\nu}$ on \mathcal{M} can be written in the form

$$g_{\mu\nu} \equiv \text{diag}(g_{AB}, R^2\gamma_{ab}), \quad (10)$$

$$T_{\mu\nu} \equiv \text{diag}(T_{AB}, QR^2\gamma_{ab}), \quad (11)$$

where g_{AB} is an arbitrary (1+1) Lorentzian metric on \mathcal{M}^2 , R a scalar on \mathcal{M}^2 , Q some function on \mathcal{M}^2 and γ_{ab} is the unit curvature metric on \mathcal{S}^2 . Note that if the background spacetime is spherically symmetric then $Q = T^a_a/2$. Here and henceforth the Greek indices denote the spacetime components, the capital Latin indices the \mathcal{M}^2 components, and the small Latin indices are used to denote the \mathcal{S}^2 components. Furthermore, the covariant derivatives on \mathcal{M} , \mathcal{M}^2 , and \mathcal{S}^2 are represented by ${}_{;\mu}$, ${}_{|A}$, and ${}_{.a}$, respectively. Finally, the totally antisymmetric covariant unit tensor on \mathcal{M}^2 is denoted as ε_{AB} and on \mathcal{S}^2 as ε_{ab} .

2. Nonradial Perturbations

As mentioned before, in this paper, we only consider axisymmetric axial parity perturbations both for the metric $\delta g_{\mu\nu}$ and the matter perturbations $\delta T_{\mu\nu}$, which are given by

$$\delta g_{\mu\nu} \equiv \begin{pmatrix} 0 & h_A^{\text{axial}} S_a^l \\ h_A^{\text{axial}} S_a^l & h(S_{a:b}^l + S_{b:a}^l) \end{pmatrix}, \quad (12)$$

$$\delta T_{\mu\nu} \equiv \begin{pmatrix} 0 & \Delta t_A^{\text{axial}} S_a^l \\ t_A^{\text{axial}} S_a^l & \Delta t(S_{a:b}^l + S_{b:a}^l) \end{pmatrix}, \quad (13)$$

where $S_a^l \equiv \varepsilon^b_a P_{l:b}$ while P_l stands for the Legendre polynomial. The gauge-invariant variables of the perturbations are then defined as

$$k_A \equiv h_A^{\text{axial}} - h_{|A} + 2h v_A, \quad (14)$$

$$L_A \equiv \Delta t_A^{\text{axial}} - Q h_A^{\text{axial}}, \quad (15)$$

$$L \equiv \Delta t - Q h, \quad (16)$$

where $v_A \equiv R_{|A}/R$ [29]. In terms of the gauge-invariant variables, the master equations for the axial parity perturbations are given by

$$k_A^{|A} = 16\pi L, \quad (17)$$

$$- \left[R^4 \left(\frac{k^A}{R^2} \right)^{|C} - R^4 \left(\frac{k^C}{R^2} \right)^{|A} \right]_{|C} + (l-1)(l+2)k^A = 16\pi R^2 L^A, \quad (18)$$

$$(R^2 L^A)_{|A} = (l-1)(l+2)L. \quad (19)$$

C. Basic equations for the magnetic field

As mentioned earlier, the electromagnetic field perturbations, $\delta F_{\mu\nu}$, are governed by the Maxwell equations, i.e.

$$\delta F_{\mu\nu,\sigma} + \delta F_{\nu\sigma,\mu} + \delta F_{\sigma\mu,\nu} = 0, \quad (20)$$

$$\delta F^{\mu\nu}{}_{;\nu} = 4\pi \delta J^\mu, \quad (21)$$

where δJ^μ is the perturbations of the current four-vector. Note that equations (20) and (21) are correct up to order of $\eta^1 \epsilon^0$. The perturbation of the electromagnetic field energy-momentum tensor, $\delta T_{\mu\nu}^{(EM)}$, in this order of approximation has the form

$$\delta T_{\mu\nu}^{(EM)} = \frac{1}{4\pi} \left(\delta F_{\mu\alpha} \delta F_{\nu\beta} g^{\alpha\beta} - \frac{1}{4} g_{\mu\nu} \delta F_{\alpha\beta} \delta F_{\lambda\gamma} g^{\alpha\lambda} g^{\beta\gamma} \right). \quad (22)$$

The electric E_μ and the magnetic field B_μ associated with the four-velocity of the fluid u^ν are defined as

$$E_\mu = \delta F_{\mu\nu} u^\nu, \quad (23)$$

$$B_\mu = \frac{1}{2} \varepsilon_{\mu\nu\alpha\beta} u^\nu \delta F^{\alpha\beta}. \quad (24)$$

Finally, we remind that in this paper we consider infinitely conductive fluids, i.e. the ideal magnetohydrodynamic approximation has been adopted, according to which $E_\mu = \delta F_{\mu\nu} u^\nu = 0$, where u^ν is the unperturbed four-velocity of the infinitely conductive fluid.

III. MAGNETIZED HOMOGENEOUS DUST COLLAPSE: FORMULATION

A. Background spacetime for perturbations

Here we briefly describe the background spacetime which will be later endowed with a magnetic field. We consider perturbations around a homogeneous spherically symmetric dust collapse described by the Oppenheimer-Snyder (OS) solution, whose line element inside the dust sphere is given by

$$ds^2 = g_{\mu\nu} dx^\mu dx^\nu, \quad (25)$$

$$= -d\tau^2 + R^2(\tau)[d\chi^2 + \sin^2 \chi(d\theta^2 + \sin^2 \theta d\phi^2)],$$

$$= R^2(\eta)[-d\eta^2 + d\chi^2 + \sin^2 \chi(d\theta^2 + \sin^2 \theta d\phi^2)], \quad (26)$$

where χ is a radial coordinate defined in the range of $0 \leq \chi \leq \chi_0$. Here χ_0 is the stellar surface and it is assumed that $\chi_0 < \pi/2$. In the line element defined earlier, $R(\eta)$ is the scale factor and $\tau(\eta)$ is the proper time of an observer comoving with the fluid, defined in terms of the conformal time η as follows

$$R(\eta) = \frac{M}{\sin^3 \chi_0} (1 + \cos \eta), \quad (27)$$

$$\tau(\eta) = \frac{M}{\sin^3 \chi_0} (\eta + \sin \eta), \quad (28)$$

where M is the total gravitational mass of the dust sphere. The energy-momentum tensor for the dust fluid is written as

$$T_{\mu\nu}^{(M)} = \rho u_\mu u_\nu, \quad (29)$$

where ρ is the rest mass density given by

$$\rho(\eta) = \frac{3 \sin^6 \chi_0}{4\pi M^2} (1 + \cos \eta)^{-3}, \quad (30)$$

and u^μ denotes the four-velocity of the dust, described in terms of comoving coordinates as

$$u^\mu = \delta^\mu_\tau \quad \text{or} \quad u^\mu = R(\eta) \delta^\mu_\eta \quad (31)$$

where δ^μ_ν means the Kronecker delta. The spacetime outside the dust sphere is described by the Schwarzschild metric, i.e.,

$$ds^2 = -f(r) dt^2 + f(r)^{-1} dr^2 + r^2 (d\theta^2 + \sin^2 \theta d\phi^2), \quad (32)$$

where $f(r) \equiv 1 - 2M/r$. From the junction conditions at the surface of the dust sphere, we obtain the relationships between the (η, χ) -coordinates and the (t, r) -coordinates, given by

$$r_s = R(\eta) \sin \chi_0, \quad (33)$$

$$\frac{t}{2M} = \ln \left| \frac{[(r_{s0}/2M) - 1]^{1/2} + \tan(\eta/2)}{[(r_{s0}/2M) - 1]^{1/2} - \tan(\eta/2)} \right| + \left(\frac{r_{s0}}{2M} - 1 \right)^{1/2} \left[\eta + \left(\frac{r_{s0}}{4M} \right) (\eta + \sin \eta) \right], \quad (34)$$

where $r_{s0} \equiv r_s(t=0) = 2M/\sin^2 \chi_0$ is the initial stellar radius in Schwarzschild coordinates.

B. The Magnetic field of the star

As mentioned earlier, we consider weakly magnetized dust spheres in which the magnetic effects on the dust fluid are treated as small perturbations on the OS solution. Moreover, for the sake of simplicity we assume that the electromagnetic fields are axisymmetric. Thus, perturbations of the electromagnetic fields, $\delta F_{\mu\nu}$, and the current four-vector, δJ_μ , can be described in terms of the Legendre polynomial P_{l_M} by the following relations

$$\delta F_{03} = -\delta F_{30} = e_1 \sin \theta \partial_\theta P_{l_M}, \quad (35)$$

$$\delta F_{13} = -\delta F_{31} = b_1 \sin \theta \partial_\theta P_{l_M}, \quad (36)$$

$$\delta F_{23} = -\delta F_{32} = b_2 \sin \theta P_{l_M}, \quad (37)$$

$$\delta F_{01} = -\delta F_{10} = e_2 P_{l_M}, \quad (38)$$

$$\delta F_{02} = -\delta F_{20} = e_3 \partial_\theta P_{l_M}, \quad (39)$$

$$\delta F_{12} = -\delta F_{21} = b_3 \partial_\theta P_{l_M}, \quad (40)$$

$$\delta J_\mu = \left(j_A P_{l_M}, j^{(p)} P_{l_M:a} + j^{(a)} S_a^{l_M} \right). \quad (41)$$

Notice, that here we have used l_M to denote the angular quantum number with respect to the electromagnetic fields to discriminate it from the one for the gravitational waves l .

In the interior of the dust sphere, the perfect conductivity condition $\delta F_{\mu\nu} u^\nu = 0$ is reduced into $\delta F_{0\mu} = 0$. This assumption leads to the following simplifications

$$e_1 = e_2 = e_3 = 0. \quad (42)$$

By direct substitution of equations (35) through (40) into the Maxwell equation (20), we obtain the basic equations describing the magnetic fields, which have the following simple form

$$\partial_\eta b_1 = \partial_\eta b_2 = \partial_\eta b_3 = 0, \quad (43)$$

$$l_M(l_M + 1)b_1 + \partial_\chi b_2 = 0. \quad (44)$$

The first of these relations, equation (43), suggests that a comoving observer does not observe any change in the magnetic field distributions. All the components of the electromagnetic fields can be determined through equations (42), (43), and (44). The Maxwell equation (21) that we still have not use can be regarded as the definition of the current four-velocity. This implies that the perturbations of the current four-velocity can be written as follows:

$$j_\eta = 0, \quad (45)$$

$$j_\chi = -\frac{l_M(l_M + 1)}{4\pi} \frac{b_3}{R^2 \sin^2 \chi}, \quad (46)$$

$$j^{(p)} = -\frac{\partial_\chi b_3}{4\pi R^2}, \quad (47)$$

$$j^{(a)} = -\frac{1}{4\pi R^2} \left(\partial_\chi b_1 + \frac{b_2}{\sin^2 \chi} \right). \quad (48)$$

The electromagnetic fields outside the star are also given by similar expressions to equations (35)–(40). In order to avoid mixing of the various quantities inside and outside the star we will indicate the ones in the exterior with a tilde i.e. \tilde{e}_1 , \tilde{b}_1 , and so on. Since the exterior of the star is vacuum, we cannot make use of the perfect conductivity condition there. Instead, we make an alternative assumption that is we demand the vanishing of the current perturbations outside the star i.e. $\delta J^\mu = 0$. This assumption simplifies considerably the Maxwell equation (21) leading into three following set of equations

$$\partial_{r_*}(r^2 \tilde{e}_2) - l_M(l_M + 1)\tilde{e}_3 = 0, \quad (49)$$

$$\partial_t(r^2 \tilde{e}_2) - l_M(l_M + 1)f\tilde{b}_3 = 0, \quad (50)$$

$$\partial_t \tilde{e}_1 - \partial_{r_*}(f\tilde{b}_1) - \frac{f}{r^2} \tilde{b}_2 = 0, \quad (51)$$

where r_* is the tortoise coordinate defined as $r_* = r + 2M \ln(r/2M - 1)$. Furthermore, from equation (20), we get a set of equations similar to equations (43) and (44), given by

$$\tilde{e}_2 - \partial_r \tilde{e}_3 + \partial_t \tilde{b}_3 = 0, \quad (52)$$

$$l_M(l_M + 1)\tilde{e}_1 + \partial_t \tilde{b}_2 = 0, \quad (53)$$

$$l_M(l_M + 1)\tilde{b}_1 + \partial_r \tilde{b}_2 = 0. \quad (54)$$

The six equations for the electromagnetic fields, i.e. equations (49) through (54), can be reduced to two decoupled wave equations

$$-\partial_t^2 \tilde{b}_2 + \partial_{r_*}^2 \tilde{b}_2 - \frac{l_M(l_M + 1)}{r^2} f \tilde{b}_2 = 0, \quad (55)$$

$$-\partial_t^2 (r^2 \tilde{e}_2) + \partial_{r_*}^2 (r^2 \tilde{e}_2) - \frac{l_M(l_M + 1)}{r^2} f (r^2 \tilde{e}_2) = 0. \quad (56)$$

Moreover, these two wave equations can be rewritten in terms of the double null coordinates, $\tilde{u} = t - r_*$ and $\tilde{v} = t + r_*$, as

$$\frac{\partial^2 \tilde{b}_2}{\partial \tilde{u} \partial \tilde{v}} + \frac{l_M(l_M + 1)}{4r^2} f \tilde{b}_2 = 0, \quad (57)$$

$$\frac{\partial^2 (r^2 \tilde{e}_2)}{\partial \tilde{u} \partial \tilde{v}} + \frac{l_M(l_M + 1)}{4r^2} f (r^2 \tilde{e}_2) = 0. \quad (58)$$

At the surface of the star, we implement the following junction conditions for the electromagnetic field

$$n^\mu B_\mu = \tilde{n}^\mu \tilde{B}_\mu, \quad (59)$$

$$q_\mu{}^\nu E_\nu = \tilde{q}_\mu{}^\nu \tilde{E}_\nu, \quad (60)$$

where n^μ , \tilde{n}^μ are the unit outward normal vector to the stellar surface defined in the interior and the exterior coordinates, respectively, while $q_\mu{}^\nu$, $\tilde{q}_\mu{}^\nu$ are the corresponding projection tensors associated with n^μ and \tilde{n}^μ . Therefore the junction conditions reduced to the following set of relations

$$b_2 = \tilde{b}_2, \quad \tilde{e}_1 + \frac{\tilde{u}^1}{\tilde{u}^0} \tilde{b}_1 = 0, \quad \tilde{e}_3 + \frac{\tilde{u}^1}{\tilde{u}^0} \tilde{b}_3 = 0, \quad (61)$$

where

$$\frac{\tilde{u}^1}{\tilde{u}^0} = \frac{\partial_\eta R}{R} f \tan \chi_0. \quad (62)$$

Concluding we mention that in this paper we focus only on dipole electromagnetic fields, i.e., electromagnetic fields associated with $l_M = 1$. Observations actually are in favor of the existence of dipole electromagnetic fields and moreover these fields can drive the quadrupole gravitational radiation as we will see in the next section. Finally, the formalism developed here accounts for electromagnetic fields which lie both inside and outside the star, in this study as a first step, we take into account only magnetic fields confined in the stellar interior. We therefore assume that $\tilde{e}_i = \tilde{b}_i = 0$ for $i = 1, 2, 3$.

C. Basic equations for the axial parity perturbations

1. Interior region of the star

As we mentioned earlier we will use the gauge-invariant formulation in the treatment of perturbations of the OS spacetime. The gauge-invariant form of axial perturbation equations (17) and (18) for the OS spacetime is reduced to the following set of equations

$$-\partial_\eta k_\eta + \partial_\chi k_\chi - 16\pi R^2 L = 0, \quad (63)$$

$$\partial_\chi (R^2 \Pi \sin^4 \chi) + (l-1)(l+2) \frac{k_\eta}{R^2} - 16\pi L_\eta \sin^2 \chi = 0, \quad (64)$$

$$\frac{1}{R^2} \partial_\eta (R^4 \Pi \sin^4 \chi) + (l-1)(l+2) \frac{k_\chi}{R^2} - 16\pi L_\chi \sin^2 \chi = 0, \quad (65)$$

where Π is the gauge-invariant quantity, defined as

$$\Pi = \frac{1}{R^2} \left[\partial_\eta \left(\frac{k_\chi}{R^2 \sin^2 \chi} \right) - \partial_\chi \left(\frac{k_\eta}{R^2 \sin^2 \chi} \right) \right]. \quad (66)$$

The regularity condition at the stellar center, suggests the introduction of a new function $\bar{\Pi}$ defined as

$$\Pi = (R \sin \chi)^{l-2} \bar{\Pi}, \quad (67)$$

which is analytic at the stellar center. By using equations (64) and (65), one can derive a single wave equation for $\bar{\Pi}$, given by

$$-\partial_\eta^2 \bar{\Pi} + \partial_\chi^2 \bar{\Pi} + 2(l+1) \left(\frac{\cos \chi}{\sin \chi} \partial_\chi \bar{\Pi} - \frac{\partial_\eta R}{R} \partial_\eta \bar{\Pi} \right) - \frac{(2l-1)(l+2)R(0)}{2R} \bar{\Pi} = \frac{16\pi}{R^l \sin^l \chi} (\partial_\chi L_\eta - \partial_\eta L_\chi), \quad (68)$$

where $R(0) = 2M/\sin^3 \chi_0$. Moreover the equation of motion (19) is rewritten as

$$-\partial_\eta (R^2 L_\eta \sin^2 \chi) + \partial_\chi (R^2 L_\chi \sin^2 \chi) = (l-1)(l+2)R^2 L. \quad (69)$$

The perturbation of the energy-momentum tensor $\delta T_{\mu\nu}$ can be splitted into two parts as shown before:

$$\delta T_{\mu\nu} = \delta T_{\mu\nu}^{(M)} + \delta T_{\mu\nu}^{(EM)}, \quad (70)$$

where $T_{\mu\nu}^{(M)}$ and $T_{\mu\nu}^{(EM)}$ are the energy-momentum tensors for the dust and the electromagnetic field, respectively. Since axial parity perturbations of the four-velocity of the fluid, δu_μ , defined as

$$\delta u_\mu = (0, 0, \beta(\tau, \chi) S_a^l), \quad (71)$$

the expansion coefficients of $\delta T_{\mu\nu}^{(M)}$ introduced in equation (13) are given by

$$\Delta t_\eta^{(M)} = \beta \rho u_\eta, \quad (72)$$

$$\Delta t_\chi^{(M)} = \Delta t^{(M)} = 0. \quad (73)$$

In this paper we constrain our study to the quadrupole gravitational radiation emitted by axial parity perturbations. The reason is that quadrupole radiation directly couples with dipole magnetic fields and it is dominant component for gravitational wave emission. As discussed before, the perturbations of the energy-momentum tensor for the electromagnetic field, $\delta T_{\mu\nu}^{(EM)}$, are of order $\sim (\delta F_{\mu\nu})^2$. Therefore, we cannot achieve separation of variables for $\delta T_{\mu\nu}^{(EM)}$ even if the background spacetime is spherically symmetric. Since we assume dipole electromagnetic fields ($l_M = 1$), then $\delta T_{\mu\nu}^{(EM)}$ will contain terms associated with $l = 0$ and $l = 2$. For the detailed calculations of various components of $\delta T_{\mu\nu}^{(EM)}$ inside the star, see Appendix A. Finally, the expansion coefficients for $\delta T_{\mu\nu}^{(EM)}$ associated with $l = 2$ are given by

$$\Delta t_\eta^{(EM)} = 0, \quad (74)$$

$$\Delta t_\chi^{(EM)} = -\frac{b_2 b_3}{12\pi R^2 \sin^2 \chi}, \quad (75)$$

$$\Delta t^{(EM)} = \frac{b_1 b_3}{12\pi R^2}. \quad (76)$$

Thus we can derive the gauge-invariant quantities for the total matter perturbations (the dust fluid and the magnetic field), L_A and L , which have the following form

$$L_\eta = -R\beta\rho, \quad (77)$$

$$L_\chi = -\frac{b_2 b_3}{12\pi R^2 \sin^2 \chi}, \quad (78)$$

$$L = \frac{b_1 b_3}{12\pi R^2}. \quad (79)$$

Substituting equations (77) through (79) into equation (69), we get the following equation of motion for β

$$\partial_\eta \beta = \frac{1}{12\pi R^3 \rho \sin^2 \chi} \left[b_2 (\partial_\chi b_3) + \left\{ 1 - \frac{(l-1)(l+2)}{2} \right\} b_3 (\partial_\chi b_2) \right], \quad (80)$$

notice that in this derivation we have used the perturbed Maxwell equation (44). Using the relations, $R^3\rho = 3R(0)/8\pi = \text{const.}$, $\partial_\eta b_2 = 0$, and $\partial_\eta b_3 = 0$, we can analytically integrate equation (80) with respect to conformal time η , to get the solution

$$\bar{\beta}(\eta, \chi) = \frac{2\eta}{9R(0)R^{l+1}\sin^{l+3}\chi} \left[b_2(\partial_\chi b_3) + \left\{ 1 - \frac{(l-1)(l+2)}{2} \right\} b_3(\partial_\chi b_2) \right] + \left(\frac{R(0)}{R} \right)^{l+1} \bar{\beta}_0(\chi), \quad (81)$$

where $\bar{\beta} = \beta/(R\sin\chi)^{l+1}$ and $\bar{\beta}_0(\chi)$ is the initial distribution of $\bar{\beta}$. Following Ref. [25], in this paper, we adopt three different definitions for the initial distribution $\bar{\beta}_0(\chi)$ i.e.

$$\bar{\beta}_0(\chi) = \mathcal{U}_1 (= \text{const.}), \quad (82)$$

$$\bar{\beta}_0(\chi) = \mathcal{U}_2 \exp \left[- \left(\frac{R(0)\sin\chi}{R_c} \right)^2 \right], \quad (83)$$

$$\bar{\beta}_0(\chi) = \mathcal{U}_3 \exp \left[- \left(\frac{R(0)\sin\chi - r_{s0}}{R_c} \right)^2 \right], \quad (84)$$

where \mathcal{U}_i is an arbitrary constant and R_c is a scale factor describing the inhomogeneity of the fluid velocity's initial distribution. Here following Ref. [25] we choose $R_c = r_{s0}/3$.

In the actual numerical calculations, we use the two null coordinates, ($u = \eta - \chi$ and $v = \eta + \chi$) and the master equation (68) is rewritten in these coordinates as

$$\frac{\partial^2 \bar{\Pi}}{\partial u \partial v} + \frac{l+1}{2} \left(\frac{\cos\chi}{\sin\chi} + \frac{\partial_\eta R}{R} \right) \frac{\partial \bar{\Pi}}{\partial u} - \frac{l+1}{2} \left(\frac{\cos\chi}{\sin\chi} - \frac{\partial_\eta R}{R} \right) \frac{\partial \bar{\Pi}}{\partial v} + \frac{(2l-1)(l+2)R(0)}{8R} \bar{\Pi} = S(\eta, \chi), \quad (85)$$

$$S(\eta, \chi) = 4\pi R^2 \rho \{ (l+1) \cos\chi \bar{\beta} + \sin\chi (\partial_\chi \bar{\beta}) \} + \frac{2b_2 b_3 (\partial_\eta R)}{3R^{l+3} \sin^{l+2}\chi}. \quad (86)$$

In summary, inside the star, our basic equations describing the gravitational perturbations are equations (85) and (86). The source term $S(\eta, \chi)$ is given uniquely by the function $\bar{\beta}(\eta, \chi)$, shown in equation (81), for a given initial distribution of the electromagnetic field and the fluid velocity perturbations.

2. Exterior region of the star

The Oppenheimer-Snyder solution (26) for the interior is matched with the Schwarzschild solution (32) for the exterior and the master equations for perturbations (17) and (18) in the interior reduce to the well known Regge-Wheeler equation in the exterior, which has the form

$$-\partial_t^2 \tilde{\Phi} + \partial_{r_*}^2 \tilde{\Phi} - \tilde{V}(r) \tilde{\Phi} = 16\pi r (\partial_{r_*} \tilde{L}_t - f \partial_t \tilde{L}_r), \quad (87)$$

$$\tilde{V}(r) = f \left(\frac{l(l+1)}{r^2} - \frac{6M}{r^3} \right), \quad (88)$$

where $\tilde{\Phi}$ is the Regge-Wheeler function, related to the gauge-invariant variable $\tilde{\Pi}$ through the relationship

$$\tilde{\Phi} = r^3 \tilde{\Pi} = r^3 \left[\partial_t \left(\frac{\tilde{k}_r}{r^2} \right) - \partial_r \left(\frac{\tilde{k}_t}{r^2} \right) \right]. \quad (89)$$

If the electromagnetic fields do not vanish outside the star, we need take into account their influence on the gravitational radiation emitted during the collapse. In the exterior the only non-vanishing contribution to the perturbations of the energy-momentum tensor $\delta \tilde{T}_{\mu\nu}$ is the one from the electromagnetic field. The expansion coefficients for $\delta \tilde{T}_{\mu\nu}$ associated with the $l=2$ axial parity perturbations are then given by the following formulae

$$\tilde{L}_t = \Delta \tilde{t}_t^{(EM)} = -\frac{1}{12\pi} \left(f \tilde{e}_2 \tilde{b}_1 + \frac{1}{r^2} \tilde{e}_3 \tilde{b}_2 \right), \quad (90)$$

$$\tilde{L}_r = \Delta \tilde{t}_r^{(EM)} = -\frac{1}{12\pi} \left(\frac{1}{f} \tilde{e}_1 \tilde{e}_2 + \frac{1}{r^2} \tilde{b}_2 \tilde{b}_3 \right), \quad (91)$$

$$\tilde{L} = \Delta \tilde{t}^{(EM)} = -\frac{1}{12\pi} \left(\frac{1}{f} \tilde{e}_1 \tilde{e}_3 - f \tilde{b}_1 \tilde{b}_3 \right). \quad (92)$$

Actually, in Appendix B, we present the detailed form of the various components of the perturbed energy-momentum tensor for the electromagnetic field outside the star.

By using the vacuum Maxwell equations (49)–(54), we can rewrite \tilde{L}_t , \tilde{L}_r , and \tilde{L} in terms of \tilde{e}_2 and \tilde{b}_2 as

$$\tilde{L}_t = \frac{f}{24\pi} \left[\tilde{e}_2(\partial_r \tilde{b}_2) - \frac{2}{r} \tilde{e}_2 \tilde{b}_2 - \tilde{b}_2(\partial_r \tilde{e}_2) \right], \quad (93)$$

$$\tilde{L}_r = \frac{1}{24\pi f} \left[\tilde{e}_2(\partial_t \tilde{b}_2) - \tilde{b}_2(\partial_t \tilde{e}_2) \right], \quad (94)$$

$$\tilde{L} = \frac{1}{48\pi} \left[2r\tilde{e}_2(\partial_t \tilde{b}_2) + r^2(\partial_t \tilde{b}_2)(\partial_r \tilde{e}_2) - r^2(\partial_t \tilde{e}_2)(\partial_r \tilde{b}_2) \right]. \quad (95)$$

Finally, the Regge-Wheeler equation (87) can be rewritten in terms of the double null coordinates, $\tilde{u} = t - r_*$ and $\tilde{v} = t + r_*$, as

$$\frac{\partial^2 \tilde{\Phi}}{\partial \tilde{u} \partial \tilde{v}} + \frac{1}{4} \tilde{V}(r) \tilde{\Phi} = \frac{f}{3r^2} \left[r^2 \tilde{e}_2(\partial_{r_*} \tilde{b}_2) - \tilde{b}_2(\partial_{r_*} r^2 \tilde{e}_2) \right], \quad (96)$$

where we have modified the right-hand side of the Regge-Wheeler equation by using equations (55) and (56). Still, since in this study we don't take into account the influence of the electromagnetic field outside the star, the right-hand side of equation (96) vanishes.

D. Junction conditions at the stellar surface

In order to ensure that the spacetime is regular at the stellar surface ($\chi = \chi_0$), we impose three junction conditions for the case of axial parity perturbations; first we demand the continuity of Π , second that $n^A \Pi|_A - 16\pi(R \sin \chi)^{-2} u^A L_A = \tilde{n}^A \tilde{\Pi}|_A - 16\pi r^{-2} \tilde{u}^A \tilde{L}_A$, and the last is $u^A \Pi|_A = \tilde{u}^A \tilde{\Pi}|_A$. These boundary conditions arise from the continuity conditions for the induced metric and the extrinsic curvature [29]. Therefore the junction conditions are explicitly given by

$$\Pi = \tilde{\Pi}, \quad (97)$$

$$\begin{aligned} -Z + W + \frac{16\pi\beta\rho}{R \sin^2 \chi_0} &= ((\partial_\eta R) \sin \chi_0 - R \cos \chi_0) \frac{\tilde{Z}}{f} + ((\partial_\eta R) \sin \chi_0 + R \cos \chi_0) \frac{\tilde{W}}{f} \\ &\quad - \frac{16\pi}{fr^2} \left(\tilde{L}_t R \cos \chi_0 + f \tilde{L}_r (\partial_\eta R) \sin \chi_0 \right), \end{aligned} \quad (98)$$

$$Z + W = (R \cos \chi_0 - (\partial_\eta R) \sin \chi_0) \frac{\tilde{Z}}{f} + (R \cos \chi_0 + (\partial_\eta R) \sin \chi_0) \frac{\tilde{W}}{f}, \quad (99)$$

where $Z = \partial \Pi / \partial u$, $W = \partial \Pi / \partial v$, $\tilde{Z} = \partial \tilde{\Pi} / \partial \tilde{u}$, and $\tilde{W} = \partial \tilde{\Pi} / \partial \tilde{v}$. The last two conditions, (98) and (99), can be rewritten as

$$W = (R \cos \chi_0 + (\partial_\eta R) \sin \chi_0) \frac{\tilde{W}}{f} - \frac{8\pi}{fr^2} \left(\tilde{L}_t R \cos \chi_0 + f \tilde{L}_r (\partial_\eta R) \sin \chi_0 \right) - \frac{8\pi\beta\rho}{R \sin^2 \chi_0}, \quad (100)$$

$$Z = (R \cos \chi_0 - (\partial_\eta R) \sin \chi_0) \frac{\tilde{Z}}{f} + \frac{8\pi}{fr^2} \left(\tilde{L}_t R \cos \chi_0 + f \tilde{L}_r (\partial_\eta R) \sin \chi_0 \right) + \frac{8\pi\beta\rho}{R \sin^2 \chi_0}. \quad (101)$$

IV. NUMERICAL PROCEDURE

In this section we describe the numerical procedures that we will follow and the way that we generate initial data. In order to simplify the numerical procedure and to set the initial data both in the interior and exterior of the collapsing configuration, we divide the background spacetime into three regions named I, II, and III, as illustrated in Fig. 1. Region I represents the stellar interior, while regions II and III the exterior spacetime. Region III is separated from region II via the null hypersurface defined by $\tilde{v} = \tilde{v}_0$, which is generated by the ingoing null rays emitted from the point where the stellar surface reaches the event horizon. Note that it is sufficient to consider the regions I, II, and III because the gray area in Fig. 1 is causally disconnected from the stellar interior at $\eta = 0$ when the magnetic fields confined inside the star. To solve the wave equation numerically, we make use of the finite differencing scheme

proposed by Hamadé and Stewart [37], in which the double null coordinates (u, v) are employed in region I and (\tilde{u}, \tilde{v}) in regions II and III, respectively. Notice that we integrate the wave equation in region I by using a first order finite differencing scheme to avoid numerical instabilities appearing near the stellar center, while Hamadé and Stewart's original scheme is of a second order finite differencing scheme.

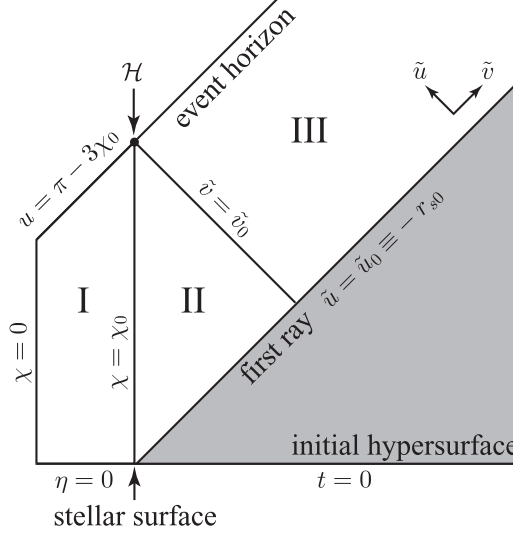


FIG. 1: A schematic description of the Oppenheimer-Snyder spacetime for the collapsing model in characteristic coordinates. Region I denotes the stellar interior while regions II and III correspond to the exterior. The stellar surface, where $r = r_s$ and $\chi = \chi_0$, is the boundary between regions I and II, and the stationary region outside star is indicated by gray.

A. Initial Data

In order to initiate the numerical calculations, we need to provide a data set on the initial hypersurface for the quantities $\bar{\Pi}$, $\partial_u \bar{\Pi}$, $\partial_v \bar{\Pi}$, $\bar{\beta}_0$, b_2 , and b_3 for the stellar interior, and $\tilde{\Phi}$, $\partial_{\tilde{u}} \tilde{\Phi}$, and $\partial_{\tilde{v}} \tilde{\Phi}$ for the stellar exterior. Following [22], we assume that the initial perturbations are “momentarily static”. Outside the star, the momentarily static initial condition for the metric perturbations is given as a static vacuum solution of equation (87) in terms of hypergeometric functions

$$\tilde{\Phi}_{\text{static}} = \frac{q_l}{l(l+1)} \left(\frac{2M}{r} \right)^l F_l \left(l-1, l+3, 2l+2; \frac{2M}{r} \right), \quad (102)$$

where q_l is a constant representing the multipole moment of the star. Here we assume that $q_l = 2M$. We remind that there is no electromagnetic field outside the star. Since it is a static solution, the initial perturbation outside the star (102) does not evolve until a light signal from the stellar interior arrives there. Finally, set the initial data i.e. the static solution (102), on the null hypersurface $\tilde{u} = \tilde{u}_0$ for the characteristic initial value problem.

As for the initial condition inside the star, we have to give a data set not only for metric perturbations but also for fluid and electromagnetic perturbations. As mentioned earlier, the initial fluid distribution $\bar{\beta}_0$ is given by equations (82)–(84), while the initial distribution for the magnetic fields b_2 , b_3 will be discussed later in §VI. Finally, the momentarily static initial data for metric perturbations $\bar{\Pi}$ in region I defined by the conditions $\partial_\eta \bar{\Pi} = 0$ and $\partial_\eta^2 \bar{\Pi} = 0$. The data sets at $\eta = 0$ for $\partial_u \bar{\Pi}$ and $\partial_v \bar{\Pi}$ are then defined via the relations $\partial_u \bar{\Pi} = -(\partial_\chi \bar{\Pi})/2$ and $\partial_v \bar{\Pi} = (\partial_\chi \bar{\Pi})/2$, respectively. The momentarily static distribution of $\bar{\Pi}(\eta = 0)$ due to the conditions $\partial_\eta \bar{\Pi} = 0$ and $\partial_\eta^2 \bar{\Pi} = 0$, is given as a regular solution of

$$\partial_\chi^2 \bar{\Pi} + 2(l+1) \frac{\cos \chi}{\sin \chi} \partial_\chi \bar{\Pi} - \frac{(2l-1)(l+2)R(0)}{2R} \bar{\Pi} = \frac{16\pi}{R^l \sin^l \chi} (\partial_\chi L_\eta - \partial_\eta L_\chi). \quad (103)$$

The regular solutions of equation (103) must be smoothly connected to the static exterior solution (102) through the stellar surface. This leads to a boundary condition for $\bar{\Pi}(\eta = 0)$ at the surface of the star described by the following

equation

$$\left(2l + 1 - \frac{rF_{l,r}}{F_l}\right) \bar{\Pi} + \tan \chi_0 \bar{\Pi}_{,\chi} + \frac{16\pi\beta\rho}{(R \sin \chi_0)^{l-1} \cos \chi_0} + \frac{16\pi\tilde{L}_t}{f(R \sin \chi_0)^{l-1}} = 0, \quad (104)$$

where F_l is the abbreviation for the hypergeometric function $F_l(l-1, l+3, 2l+2; 2M/r)$. Finally, the regularity at the stellar center requires that the function $\bar{\Pi}$ is analytic for $\chi \rightarrow 0$.

B. Boundary Conditions

The boundary conditions for the numerical integration are the regularity condition at the stellar center and that there are no incoming waves at the infinity. The regularity condition at the stellar center demands that $\partial_\chi \bar{\Pi} = 0$, which is reduced to

$$\frac{\partial \bar{\Pi}}{\partial u} = \frac{\partial \bar{\Pi}}{\partial v}. \quad (105)$$

Finally, for the no incoming radiation condition at the infinity, we adopt the condition $\partial \tilde{\Phi} / \partial \tilde{u} = 0$ (see, e.g., [37]).

C. Special Treatment of the Junction Conditions near the Event Horizon

When the stellar surface reaches the event horizon, the junction conditions discussed earlier in §III D cannot be used any more because the terms related to f^{-1} diverge. Instead of these junction conditions, following [25], we impose the following junction conditions on the null surface of $\tilde{v} = \tilde{v}_0$ in the vicinity of the point \mathcal{H} in Fig. 1:

$$\Pi = \Pi^{N_{\max}} + \frac{\Pi^{\text{EH}} - \Pi^{N_{\max}}}{r^{\text{EH}} - r^{N_{\max}}} (r - r^{N_{\max}}), \quad (106)$$

$$\Pi^{\text{EH}} \equiv \Pi^{N_{\max}} + \frac{\Pi^{N_{\max}} - \Pi^{N_{\max}-1}}{r^{N_{\max}} - r^{N_{\max}-1}} (r^{\text{EH}} - r^{N_{\max}}), \quad (107)$$

where Π^n and r^n are the values of Π and r on $\tilde{v} = \tilde{v}_0$ at n -th time steps, while N_{\max} denotes the total number of time steps in region II, and $r^{\text{EH}} = 2M$.

V. CODE TESTS

In order to check our numerical code, we have calculated the quadrupole gravitational radiation emitted during the collapse of a non-magnetized homogeneous dust sphere (perturbations of the Oppenheimer-Snyder solution), which has been already studied by several authors, e.g., [22, 25]. For the test we will consider the collapse of the homogeneous dust sphere which is initially at rest. Therefore, we have to provide the initial radius of the dust sphere to begin the numerical integration. Since the amount of gravitational radiation emitted during the collapse of a non-magnetized homogeneous dust sphere is the ‘‘typical value’’ with which we will compare the energy emitted during the collapse of a magnetized homogeneous dust sphere, we will briefly summarize these results.

In the present calculations, the number of the spatial grid points inside the star (region I) is chosen to be $N_\chi = 1000$. Using this number of grid points we manage to obtain numerical solutions and results with acceptable accuracy. In region III, the step-size for integration is determined by the relation $\Delta \tilde{u} = (u_{\max} - u_0) / N_{\tilde{u}}$, where $u_{\max} \equiv t_{\max} - r_{*\text{ob}}$. Here, t_{\max} is the expected maximum time for observation and $r_{*\text{ob}}$ is the position of the observer described in tortoise coordinate units. In this paper, we assume that $t_{\max} = 2000M$ while the fiducial observer is at $r_{\text{ob}} = 40M$.

As a first step we confirm the convergence of our numerical code. For this purpose, by varying the value of $N_{\tilde{u}}$, we calculate the total energy radiated in gravitational waves during the collapse which will be characterized by the initial radius of the dust sphere, $r_{s0} = 8M$, and the $\beta_0 = \text{const.}$ velocity distribution. The radiated energy is estimated by integrating the luminosity of gravitational waves $L_{GW,l}$ with respect to time. Here, the luminosity $L_{GW,l}$ of gravitational waves is defined by the relation (see, e.g., [22, 25])

$$L_{GW,l} = \frac{1}{16\pi} \frac{l(l+1)}{(l-1)(l+2)} (\tilde{\Phi}_{,\tilde{u}})^2. \quad (108)$$

The outcome of this calculation i.e. the energy emitted in gravitational waves during the collapse as a function of $N_{\tilde{u}}$ is shown in Fig. 2 and tabulated in Table I. From Fig. 2 we conclude that the amount of the total energy emitted during the collapse converges for $N_{\tilde{u}} \geq 10000$, thus we assumed in all numerical runs $N_{\tilde{u}} = 10000$. In Fig. 3, we give the relative error in the total emitted energy obtained by our numerical code as a function of $\Delta\tilde{u}$. Here, the quantity $= (E(\Delta\tilde{u}) - E_m)/E_m$ stands for the relative error, then $E(\Delta\tilde{u})$ denotes the total energy emitted for various values of $\Delta\tilde{u}$ and E_m is the energy for some maximum value $N_{\tilde{u}} = 20000$. It is obvious from Fig. 3 that our numerical code achieves second order accuracy.

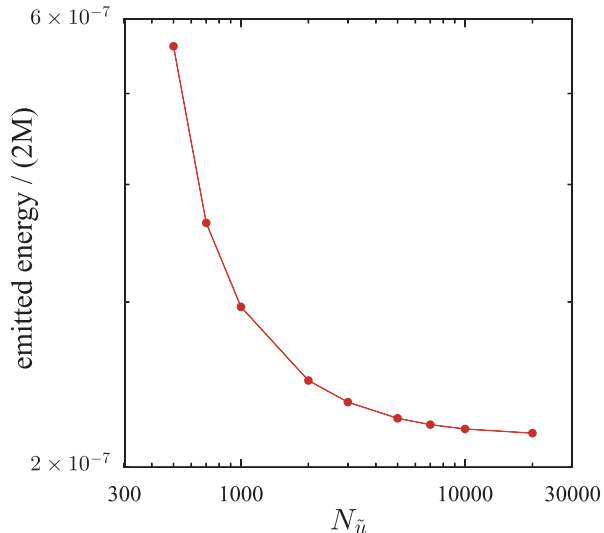


FIG. 2: The total radiated energy of quadrupole gravitational waves from the OS collapse characterized by the initial radius of the dust sphere $r_{s0} = 8M$ and $\tilde{\beta}_0 = const.$ velocity distribution, as function of the number of grid points in region III.

TABLE I: The total radiated energies of quadrupole gravitational waves from the collapse characterized by the initial radius of the dust sphere $r_{s0} = 8M$ and the $\tilde{\beta}_0 = const.$ velocity distribution.

$N_{\tilde{u}}$	$\Delta\tilde{u}$	emitted energy / (2M)
500	$3.929M$	5.614×10^{-7}
700	$2.806M$	3.641×10^{-7}
1000	$1.964M$	2.964×10^{-7}
5000	$0.3929M$	2.255×10^{-7}
10000	$0.1964M$	2.197×10^{-7}
20000	$0.09822M$	2.175×10^{-7}

Next, let us compare the total energy emitted during the collapse as it has been calculated by our numerical code with the results by Cunningham, Price, and Moncrief [22] (CPM1978). In Fig. 4, we show the total energy emitted in gravitational waves during the collapse as function of the initial radius of the dust sphere r_{s0} . In this figure, the results of CPM1978 are indicated by the filled-squares, while the other symbols represent our results. The results for the initial distribution of the fluid velocity defined by equation (82) are indicated by circles, those defined by equation (83) are indicated by triangles while for the distribution defined by equation (84) we used squares. Finally, the results obtained by using a numerical code with the first order accuracy, are indicated by the gray asterisks. This figure shows that there are small differences between our results and those obtained by CPM1978. We however observe that the results of CPM1978 agree well with those with the first order accuracy (compare the filled-squares with the asterisks). Therefore, we conclude that our results are in quite good agreement with the results of CPM1978.

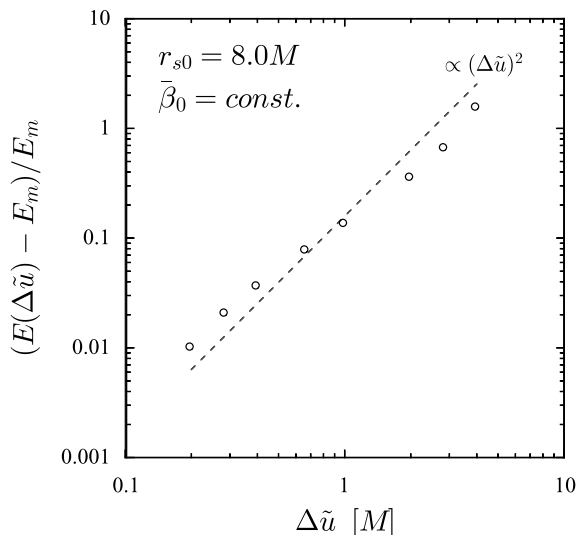


FIG. 3: Convergence test of the numerical code. The vertical axis denotes the “relative error”, that is the ratio of $E(\Delta\tilde{u}) - E_m$ over E_m , where $E(\Delta\tilde{u})$ is the emitted energy for various of $\Delta\tilde{u}$ and E_m is the energy for $N_{\tilde{u}} = 20000$. The dashed line is $\propto (\Delta\tilde{u})^2$ suggesting that as $\Delta\tilde{u}$ becomes smaller the “relative error” reduces as $(\Delta\tilde{u})^2$.

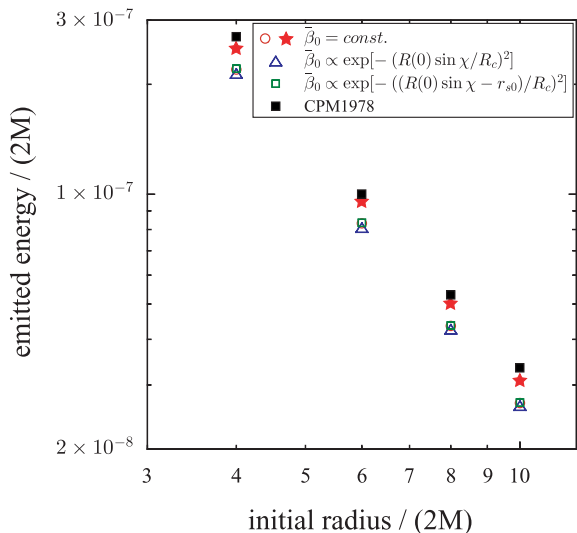


FIG. 4: The energy emitted in gravitational waves from the homogeneous dust collapse without magnetic field as a function of the initial stellar radius where $r_{s0} = 8M, 12M, 16M,$ and $20M$. The filled-squares correspond to the results by [22] while the rest correspond to our results. The different marks corresponds to different initial distribution $\bar{\beta}_0$. The asterisks correspond to numerical results taken by a first order code.

In Fig. 5, we show the waveforms of the quadrupole gravitational radiation from the collapse with an initial radius $r_{s0} = 8M$ and for three different initial distributions of the fluid velocity $\bar{\beta}_0$ defined by equations (82), (83), and (84). In this figure, the left panel displays the waveforms as functions of the time, while the right panel displays the absolute values of the amplitudes as functions of the time in a log-log plot. Fig. 5 shows that the first part of the waveform is characterized by the quasinormal ringing while at the late times follows a power-law tail, as found in [22]. (For a review of quasinormal modes for compact objects, see, e.g. [38].) From the waveforms, we estimate the frequency of the fundamental quasinormal mode to be $2M\omega = 0.746 + 0.179i$, which agrees very well with the quasinormal mode frequency estimated by Chandrasekhar and Detweiler [39]. As for the late-time tail of the gravitational waves, in the right panel of Fig. 5, we find that the amplitude decays as t^{-7} at late times, which is in good agreement with the analytical estimate of Price [40], that is $t^{-(2l+3)}$. The accuracy in the estimates of the quasinormal mode

frequency and the late-time tail therefore suggest that our numerical code is accurate and reproduces all previously known results.

Besides the tests of the code the following basic properties of the gravitational radiation emitted during the collapse of the non-magnetized homogeneous dust should be emphasized. First, as it shown in Fig. 4, the total radiated energy does not critically depend on the distribution of $\bar{\beta}_0$, this has been also observed in CPM1978 and second, as shown in Fig. 5, that small modulations appear just after the onset of the collapse only for the case of $\bar{\beta}_0 \propto \exp[-(R(0) \sin \chi/R_c)^2]$.

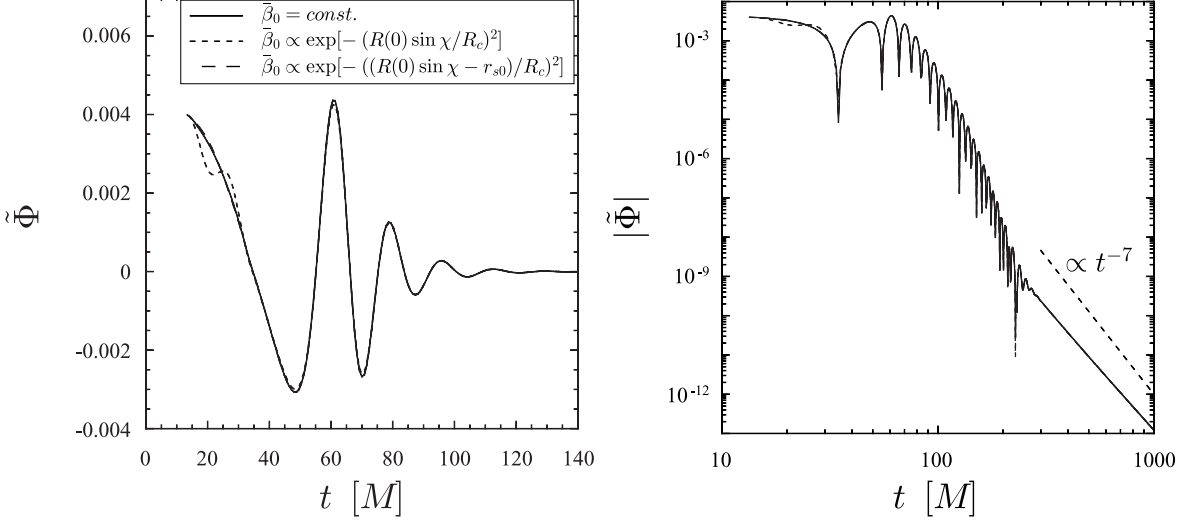


FIG. 5: The waveform of the quadrupole gravitational radiation emitted during the collapse of the non-magnetized homogeneous dust, as function of time. The initial radius of the dust sphere is set to $r_{s0} = 8M$ while the fiducial observer is set at $r = 40M$. In the right panel the amplitudes of the gravitational waves are shown in a log-log plot and the late-time is compared with its theoretical value $t^{-(2l+3)}$. Three initial distributions of the fluid velocity $\bar{\beta}_0$ were adopted and one can hardly trace their influence on the waveform.

VI. GRAVITATIONAL RADIATION FROM THE COLLAPSE OF THE HOMOGENEOUS MAGNETIZED DUST SPHERE

A. Initial distribution of the magnetic field and magnetic effects on the gravitational radiation

For the calculation of the gravitational waves emitted during the collapse of a magnetized dust sphere, one needs to provide the initial distribution (profile) of the magnetic fields, i.e., to set up the functional forms of b_2 and b_3 on the hypersurface $\eta = 0$. In practice, one has the freedom in choosing the initial distribution of b_2 and b_3 as the following two conditions are satisfied: (i) the regularity condition at the stellar center, (ii) the junction condition (61) at the stellar surface. Since here we made the assumption that the magnetic field is confined inside the star, the second condition is reduced to $b_2(\chi_0) = 0$. In this work we assume a dipole magnetic field, and for this specific geometry it is convenient to introduce two new quantities for the description of the magnetic field, \bar{b}_2 and \bar{b}_3 , defined as

$$b_2(\chi) = (R \sin \chi)^2 \bar{b}_2(\eta, \chi), \quad (109)$$

$$b_3(\chi) = (R \sin \chi)^3 \bar{b}_3(\eta, \chi). \quad (110)$$

If the new variables $\bar{b}_2(\eta, \chi)$ and $\bar{b}_3(\eta, \chi)$ are analytic at $\chi = 0$, the regularity condition at the stellar center for the magnetic field is automatically satisfied. Then for quadrupole perturbations ($l = 2$), the source term in the wave equation, $S(\eta, \chi)$, and the perturbation for the four-velocity $\bar{\beta}(\eta, \chi)$ are given by the following expressions:

$$S(\eta, \chi) = 4\pi R^2 \rho \left\{ 3\bar{\beta} \cos \chi + (\partial_\chi \bar{\beta}) \sin \chi \right\} - \frac{R(0) \sin \eta}{3} \left(\frac{R(0)}{R} \right)^5 \mathcal{B}_2 \mathcal{B}_3 \bar{b}_{20} \bar{b}_{30} \sin \chi, \quad (111)$$

$$\bar{\beta}(\eta, \chi) = \frac{2\eta R^2}{9R(0)} \left(\frac{R(0)}{R} \right)^5 \mathcal{B}_2 \mathcal{B}_3 \left\{ \bar{b}_{20} \bar{b}_{30} \tan \chi + \bar{b}_{20} (\partial_\chi \bar{b}_{30}) - (\partial_\chi \bar{b}_{20}) \bar{b}_{30} \right\} + \left(\frac{R(0)}{R} \right)^3 \bar{\beta}_0(\chi), \quad (112)$$

where \bar{b}_{20} , \bar{b}_{30} are dimensionless functions of χ , defined as

$$\bar{b}_2(\eta, \chi) = \left(\frac{R(0)}{R}\right)^2 \mathcal{B}_2 \bar{b}_{20}(\chi), \quad (113)$$

$$\bar{b}_3(\eta, \chi) = \left(\frac{R(0)}{R}\right)^3 \mathcal{B}_3 \bar{b}_{30}(\chi). \quad (114)$$

Here \mathcal{B}_2 and \mathcal{B}_3 are arbitrary constants related to the strength of the magnetic field. It should be emphasized that, as shown in equations (111) and (112), all terms related to the magnetic fields in the source term $S(\eta, \chi)$ vanish when $\eta = 0$. In other words, the magnetic field does not affect the momentarily static initial data for metric perturbations. The geometry of the magnetic fields when the collapse sets in is practically unknown. Based on this freedom we adopted the following two types for the initial distribution of the magnetic field:

$$(I) : \bar{b}_{20}(\chi) = 1 - 2 \left(\frac{\chi}{\chi_0}\right)^2 + \left(\frac{\chi}{\chi_0}\right)^4, \quad \bar{b}_{30}(\chi) = 1 - \left(\frac{\chi}{\chi_0}\right)^4, \quad (115)$$

$$(II) : \bar{b}_{20}(\chi) = \bar{b}_{30}(\chi) = 4 \left[\left(\frac{\chi}{\chi_0}\right)^2 - \left(\frac{\chi}{\chi_0}\right)^4 \right]. \quad (116)$$

Note that the maximum value of \bar{b}_{20} and \bar{b}_{30} are chosen to be one in the interval $0 \leq \chi \leq \chi_0$. For the first profile function (I) the magnetic field is stronger in the center of the sphere while for profile function (II) the field becomes stronger in the outer region.

It is more convenient to explore the effects of the magnetic field on the efficiency of the gravitational radiation emission during the collapse, if one introduces the dimensionless parameter α , defined as

$$\alpha = \frac{R(0)\mathcal{B}_2\mathcal{B}_3}{\mathcal{U}_1}. \quad (117)$$

Then the source term in the wave equation, $S(\eta, \chi)$, can be split as follows

$$S = S^{(\beta)} + \alpha S^{(B)}, \quad (118)$$

where

$$S^{(\beta)} = 4\pi R(0)^2 \rho \left(\frac{R(0)}{R}\right) \{3\bar{\beta}_0 \cos \chi + (\partial_\chi \bar{\beta}_0) \sin \chi\}, \quad (119)$$

$$S^{(B)} = \mathcal{U}_1 \left(\frac{R(0)}{R}\right)^5 \left[\frac{8\pi}{9R(0)^2} R^4 \rho \eta \frac{1}{\sin^2 \chi} \partial_\chi \left\{ \left(\bar{b}_{20} \bar{b}_{30} \tan \chi + \bar{b}_{20} (\partial_\chi \bar{b}_{30}) - (\partial_\chi \bar{b}_{20}) \bar{b}_{30} \right) \sin^3 \chi \right\} - \frac{\sin \eta}{3} \bar{b}_{20} \bar{b}_{30} \sin \chi \right]. \quad (120)$$

Note that $S^{(\beta)}$ can be attributed to the incompressible fluid flow while $S^{(B)}$ to the Maxwell stress in the magnetized dust sphere. The splitting of the source term introduced with equation (118) suggests that any solution of the wave equations (85) and (96) can be expressed as a linear superposition of the two solutions, $\tilde{\Phi}^{(\beta)}$ and $\tilde{\Phi}^{(B)}$, that are independent of α , i.e.

$$\tilde{\Phi} = \tilde{\Phi}^{(\beta)} + \alpha \tilde{\Phi}^{(B)}, \quad (121)$$

where $\tilde{\Phi}^{(\beta)}$ is the solution in the absence of magnetic field ($\alpha = 0$) and $\tilde{\Phi}^{(B)}$ is the solution for the case of $S = S^{(B)}$ i.e. when the gravitational field is initially stationary. Since we assume that the initial profile of the gravitational perturbations does not depend on the existence of magnetic fields, the initial values of $\tilde{\Phi}^{(B)}$ were set to zero.

These assumptions, i.e. the splitting introduced by equations (118) and (121), suggest modifications in the form of equation (108) describing the luminosity in gravitational waves which gets the following form:

$$L_{GW,l} = \frac{1}{16\pi} \frac{l(l+1)}{(l-1)(l+2)} \{ (\tilde{\Phi}_{,\tilde{u}}^{(\beta)})^2 + \alpha^2 (\tilde{\Phi}_{,\tilde{u}}^{(B)})^2 + 2\alpha (\tilde{\Phi}_{,\tilde{u}}^{(\beta)}) (\tilde{\Phi}_{,\tilde{u}}^{(B)}) \}. \quad (122)$$

While the radiated energy in gravitational waves during the collapse is then given by following relation

$$E_{GW,l} = E_{GW,l}^{(\beta)} + \alpha^2 E_{GW,l}^{(B)} + 2\alpha C_{GW,l}, \quad (123)$$

where $E_{GW,l}^{(\beta)}$ and $E_{GW,l}^{(B)}$ stand for the total radiated energies associated with the solutions $\tilde{\Phi}^{(\beta)}$ and $\tilde{\Phi}^{(B)}$, respectively, and $C_{GW,l}$ is an integral quantity defined by the product of $\tilde{\Phi}^{(\beta)}$ and $\tilde{\Phi}^{(B)}$. Their detailed form is:

$$E_{GW,l}^{(\beta)} = \frac{1}{16\pi} \frac{l(l+1)}{(l-1)(l+2)} \int_{\tilde{v}=\tilde{v}_{max}} (\tilde{\Phi}_{,\tilde{u}}^{(\beta)})^2 d\tilde{u}, \quad (124)$$

$$E_{GW,l}^{(B)} = \frac{1}{16\pi} \frac{l(l+1)}{(l-1)(l+2)} \int_{\tilde{v}=\tilde{v}_{max}} (\tilde{\Phi}_{,\tilde{u}}^{(B)})^2 d\tilde{u}, \quad (125)$$

$$C_{GW,l} = \frac{1}{16\pi} \frac{l(l+1)}{(l-1)(l+2)} \int_{\tilde{v}=\tilde{v}_{max}} (\tilde{\Phi}_{,\tilde{u}}^{(\beta)})(\tilde{\Phi}_{,\tilde{u}}^{(B)}) d\tilde{u}. \quad (126)$$

where \tilde{v}_{max} is the maximum value of \tilde{v} .

It is worth mentioning the following issue emerging from the study of equation (123). It can be easily proved that since $E_{GW,l}$ is a quadratic function of α and $E_{GW,l}^{(B)} > 0$ then by definition, $E_{GW,l}$ gets its minimum value, $E_{GW,l}^{(min)} = E_{GW,l}^{(\beta)} - C_{GW,l}^2/E_{GW,l}^{(B)}$, for $\alpha = \alpha_c$, where $\alpha_c = -C_{GW,l}/E_{GW,l}^{(B)}$. In other words, phase cancellation between the two components $\tilde{\Phi}^{(\beta)}$ and $\tilde{\Phi}^{(B)}$ of the gravitational perturbations become maximal around $\alpha = \alpha_c$. As discussed earlier in §V, $E_{GW,l}^{(\beta)}$ does not highly depend on the initial profile of the fluid velocity. Thus, the total radiated energy $E_{GW,l}$ practically depends on α and the initial radius of the dust sphere, r_{s0} , but not on $\tilde{\beta}_0$.

B. Numerical results for the initial magnetic field profile (I)

The numerical study for the influence of the magnetic field on the gravitational wave output during the OS collapse, we have mentioned earlier, that we used two quite different initial profiles for the magnetic field. These two profiles described by the equations (115) and (116) and represent magnetic fields which have their maximum either at the stellar center or near the surface.

We first consider the case (I), given by equation (115). As discussed in the previous subsection, the fundamental quantities for estimating the gravitational radiation from the collapse of the magnetized homogeneous dust sphere are $\tilde{\Phi}^{(\beta)}$ and $\tilde{\Phi}^{(B)}$. It is obvious that we can obtain solutions of equations (85) and (96) for any value of α in terms of $\tilde{\Phi}^{(\beta)}$ and $\tilde{\Phi}^{(B)}$ through the relationship (121). In Fig. 6, we show the waveforms $\tilde{\Phi}^{(\beta)}$ and $\tilde{\Phi}^{(B)}$ of the quadrupole gravitational radiation from the collapse characterized by an initial radius $r_{s0} = 8M$ and an initial distribution of the fluid velocity $\tilde{\beta}_0 = const$. We observe in Fig. 6 that the two waveforms, $\tilde{\Phi}^{(\beta)}$ and $\tilde{\Phi}^{(B)}$, are almost in phase. Therefore, we expect the following properties of the gravitational wave amplitude: (1) for $\alpha > 0$, as α increases, the gravitational wave amplitude $\tilde{\Phi}$ increases monotonically and the phase of $\tilde{\Phi}$ does not change, (2) for $\alpha < 0$, as α decreases, the amplitude and phase of the gravitational wave amplitude $\tilde{\Phi}$ show a more involved behavior due to the phase cancellation between the two gravitational wave amplitudes $\tilde{\Phi}^{(\beta)}$ and $\tilde{\Phi}^{(B)}$. It has been also found that the amplitude of the emitted gravitational waves is almost independent from the functional form of $\tilde{\beta}_0$ in agreement with our previous results for the non-magnetized collapse (see Fig. 5).

In Figure 7 we show the waveforms for a number of positive and negative values of α i.e. for $\alpha = -9, -6, -3, 3, 6$, and 9 . We also show, in every panel, the shape of the waveform in the absence of magnetic field ($\alpha = 0$) with a bold line. This figure verifies the previously referred theoretical estimations i.e. that for $\alpha > 0$, the phase of the various waveforms is almost the same as that of $\alpha = 0$ and the amplitude becomes larger as α increases. The amplitude of the waveforms is considerably smaller for $\alpha < 0$, due to the phase cancellation effects, and decreases for smaller values of $|\alpha|$ on the other hand the phase shift is significant for large values of $|\alpha|$. Finally, one can easily observe that the dependence of the amplitude on the initial profile of $\tilde{\beta}_0$ is very weak. Moreover, we observe another effect related to the magnetic field i.e. there is a wave packet the actual quasinormal ringing. The appearances of this wave packet can be only attributed to the functional form of $\tilde{\Phi}^{(B)}$.

As it has been argued earlier, the total energy emitted in gravitational waves during the collapse of a magnetized dust sphere for any value of α can be calculated as a proper combination of the quantities $E_{GW,l}^{(\beta)}$, $E_{GW,l}^{(B)}$, and $C_{GW,l}$ via equation (123). The values of $E_{GW,2}^{(\beta)}$, $E_{GW,2}^{(B)}$, and $C_{GW,2}$ with $\tilde{\beta}_0 = const$. for four different initial radius of the dust sphere ($r_{s0} = 8M, 12M, 16M, 20M$) are summarized in Table II. By studying equation (123) we observe that the total energy emitted in gravitational waves has a minimum for collapsing models with $\alpha = \alpha_c < 0$. Since $E_{GW,2}^{(\beta)}$'s are almost independent from the initial distribution of the fluid velocity $\tilde{\beta}_0$, as shown in Fig. 4, the total emitted energy hardly depends on $\tilde{\beta}_0$. These features can be seen in Fig. 8 where the total energy emitted in gravitational waves from the collapse is studied as function of α .

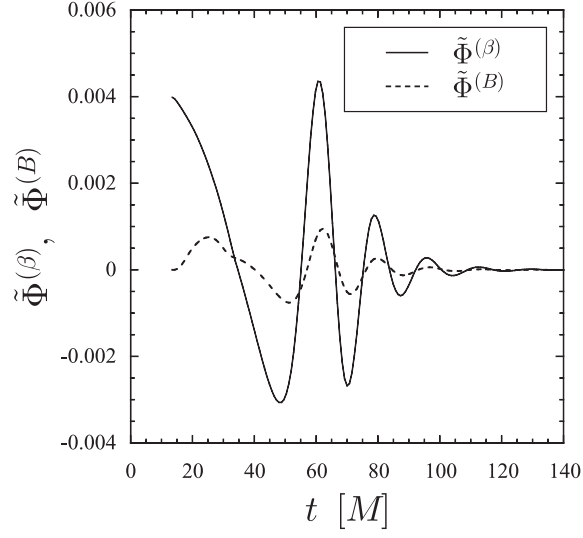


FIG. 6: The amplitude of quadrupole gravitational waves emitted during the collapse. The continuous line stands for the function $\tilde{\Phi}^{(\beta)}$ and the dashed for $\tilde{\Phi}^{(B)}$. The efficiency of the collapse depends on the initial radius of the dust sphere $r_{s0} = 8M$, the initial profile of the fluid velocity $\tilde{\beta}_0 = \text{const.}$, and the initial profile of the magnetic field, here is the case (I). The waveforms are monitored at $r = 40M$.

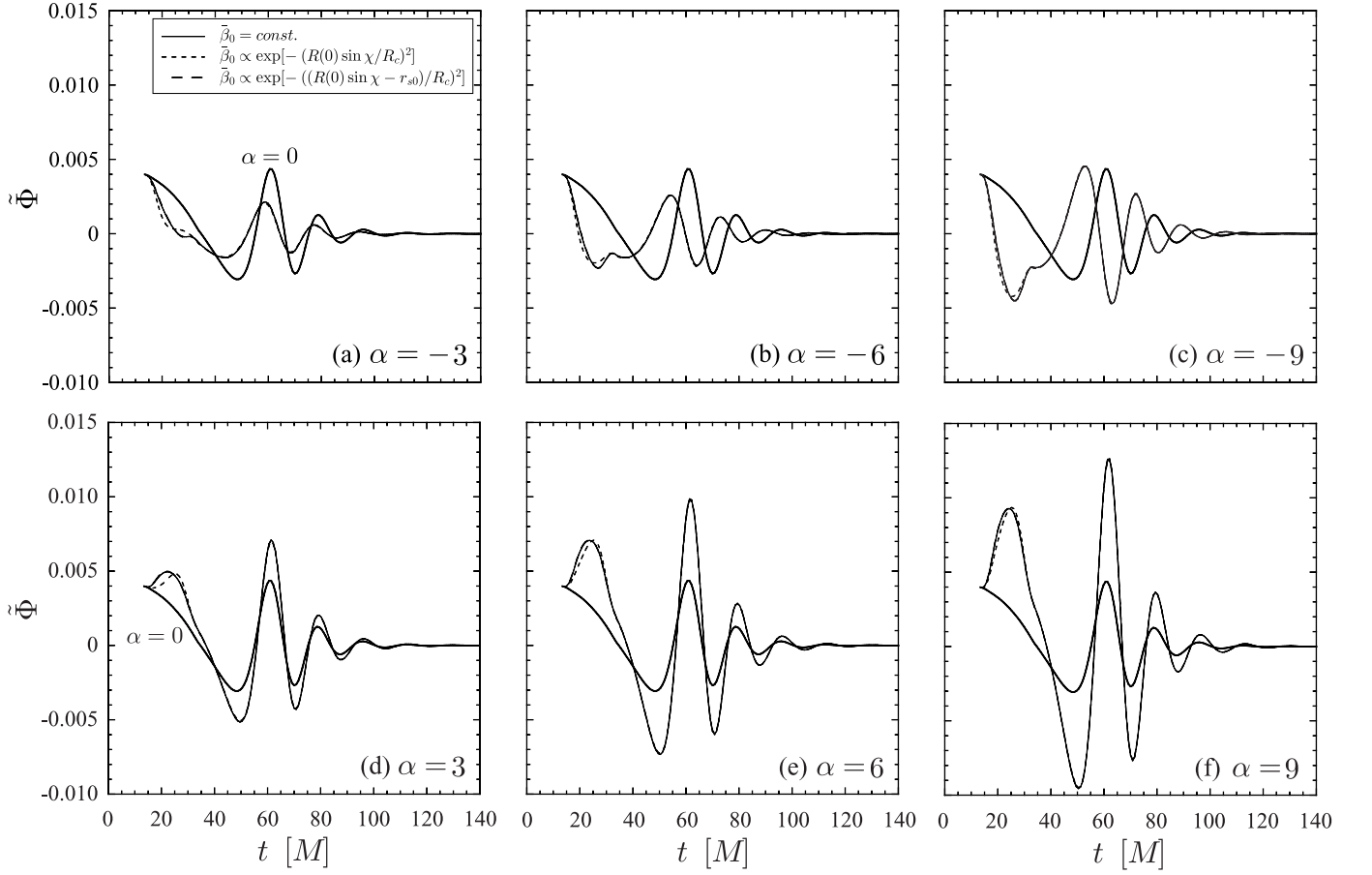


FIG. 7: Waveforms for gravitational radiation emitted during the collapse of a magnetized homogeneous dust sphere with initial radius $r_{s0} = 8M$ and initial distribution of the fluid velocity $\tilde{\beta}_0 = \text{const.}$. The gravitational waveforms are monitored at $r = 40M$. The thick continuous line corresponds to the waveform of the non-magnetized collapse ($\alpha = 0$).

The most important conclusion that can be drawn from this figure is that the total energy emitted in gravitational waves from the magnetized dust collapse can be about eleven times higher than the energy of the non-magnetized collapse for $\alpha = 10$ and about five times smaller for $\alpha = \alpha_c$. Thus, the effect of the magnetic field in the gravitational wave outcome during the collapse can be significant and might improve the possibility of detecting gravitational waves from this type of sources.

TABLE II: The values of $E_{GW,l}^{(\beta)}$, $E_{GW,l}^{(B)}$, and $C_{GW,l}$ for quadrupole gravitational waves ($l = 2$) emitted during the dust collapse for four values of the initial radius of the dust sphere ($r_{s0} = 8M$, $12M$, $16M$, and $20M$) while we assumed that $\bar{\beta}_0 = const.$ The value, $\alpha_c \equiv -C_{GW,2}/E_{GW,2}^{(B)}$, i.e. the minimum of the emitted energy $E_{GW,2}$ is also shown.

	$r_{s0} = 8M$	$r_{s0} = 12M$	$r_{s0} = 16M$	$r_{s0} = 20M$
$E_{GW,2}^{(\beta)}/(2M)$	2.197×10^{-7}	8.319×10^{-8}	4.354×10^{-8}	2.676×10^{-8}
$E_{GW,2}^{(B)}/(2M)$	1.296×10^{-8}	7.527×10^{-9}	5.557×10^{-9}	4.472×10^{-9}
$C_{GW,2}/(2M)$	4.722×10^{-8}	2.366×10^{-8}	1.501×10^{-8}	1.066×10^{-8}
α_c	-3.64	-3.14	-2.70	-2.38

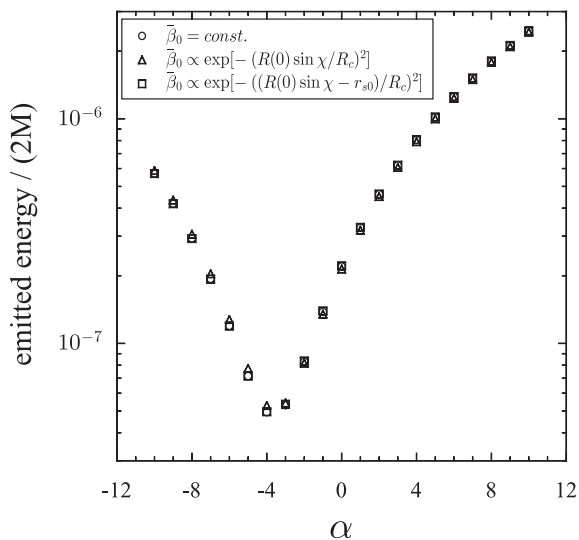


FIG. 8: The total energy emitted in gravitational waves ($l = 2$) during the homogeneous dust collapse with magnetic field as function of α . The horizontal axis denotes the value of the parameter α representing the strength of the magnetic field, while the initial radius of the sphere assumed to be $r_{s0} = 8M$.

Next we examine the dependence of the total energy emitted during the collapse on the initial radius r_{s0} of the dust sphere assuming again that the initial profile of the fluid velocity is $\bar{\beta}_0 = const.$ In Fig. 9, the waveforms from the collapse with an initial radius $r_{s0} = 20M$ are shown. From this figure, can be easily seen that the effect of the magnetic field becomes more pronounced as the initial stellar radius increases while the basic properties (dependence on α and phase shift) are similar to those of the $r_{s0} = 8M$ case. The influence of the magnetic field in the gravitational wave output increases with increasing radius, a natural explanation is that the longer the collapse lasts the longer the magnetic field will influence the dynamics of the collapsing dust. Actually, if the collapsing sphere has an initial radius $r_{s0} = 8M$ then it takes $t \sim 50M$ until one observes the first peak of the quasinormal ringing, while it takes $t \sim 140M$ for the $r_{s0} = 20M$ model. Additionally, we can observe that a wave packet before the quasinormal ringing is suppressed, compare with Fig. 6.

In Figure 10, we show the total energy emitted in gravitational waves as a function of α for several values of the initial radius of the dust sphere. From this figure, we can see that the critical value α_c , increases as r_{s0} increases, see also Table II, while the emitted energy decreases as r_{s0} increases. However the effect of magnetic field is stronger for the model with larger initial radius, i.e., the emitted energy varies with the strength of the magnetic field. Actually,

as we mentioned earlier the ratio of the energy of the magnetized collapse over the energy of the non-magnetized one varies from 0.22 ($\alpha = \alpha_c$) to 11.2 ($\alpha = 10$) for $r_{s0} = 8M$. For $r_{s0} = 20M$ the same ratio varies from 0.050 (at $\alpha = \alpha_c$) to 25.7 (at $\alpha = 10$).

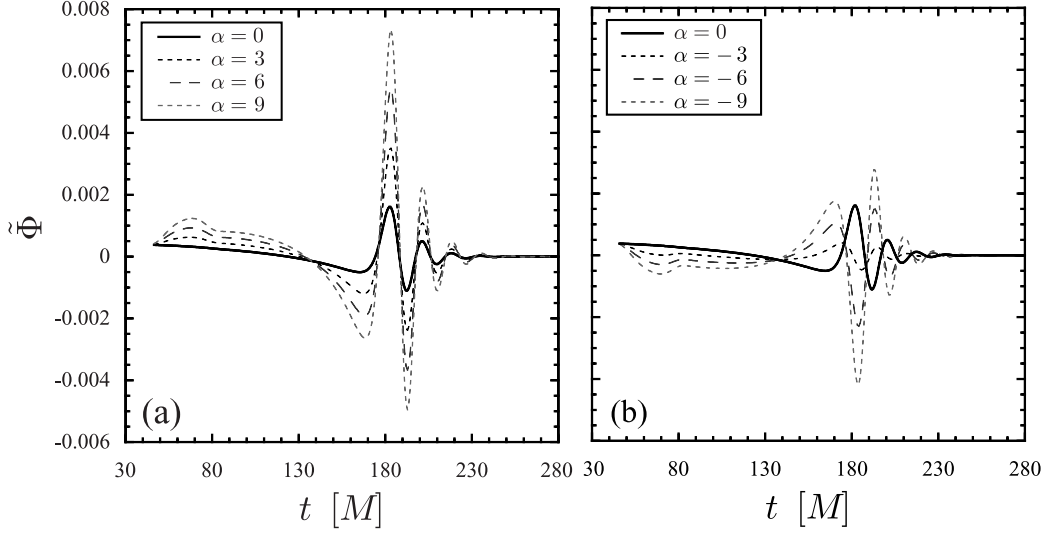


FIG. 9: Waveform of gravitational waves for $l = 2$ for (a) $\alpha \geq 0$ and (b) $\alpha \leq 0$. The initial radius is $r_{s0} = 20M$ while the observer is set at $r = 40M$ and we also assume that $\bar{\beta}_0 = const.$

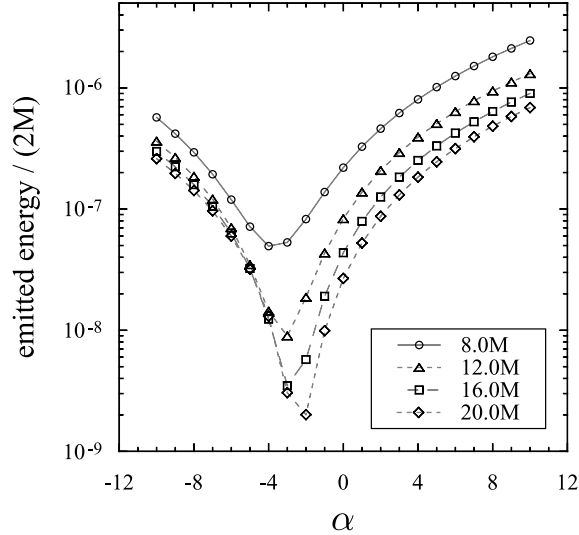


FIG. 10: The total energy emitted in gravitational waves ($l = 2$) from the homogeneous dust collapse with magnetic field for four values of initial radius $r_{s0} = 8M, 12M, 16M,$ and $20M$ as function of the magnetic field strength.

C. Numerical results for the initial magnetic field profile (II)

The second magnetic field profile considered in this work is the one that has its maximum close to the stellar surface and is described by equation (116). Here, again we assumed an initial profile for the fluid velocity that has $\bar{\beta}_0 = const.$ and the initial radius of the dust sphere is set to $r_{s0} = 8M$. In Fig. 11, we show the two components of the waveforms

$\tilde{\Phi}^{(\beta)}$ and $\tilde{\Phi}^{(B)}$ for profiles (I) and (II). From this figure, we can see that the phase of $\tilde{\Phi}^{(B)}$ is almost independent of the initial profile of the magnetic field while the amplitude of the gravitational wave associated with the profile (II) is smaller than the one associated with the profile (I).

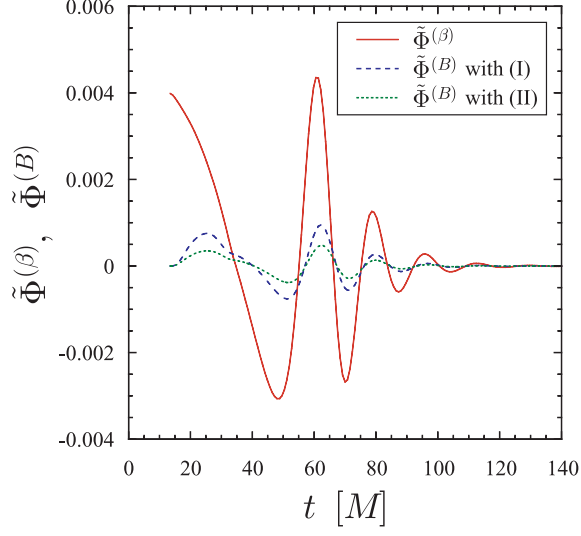


FIG. 11: Waveforms of quadrupolar gravitational radiation from the magnetized OS collapse associated with $\tilde{\Phi}^{(\beta)}$ and $\tilde{\Phi}^{(B)}$, for the two initial profiles (I and II) for the magnetic field.

In Fig. 12, we compare the total energy emitted in gravitational waves as functions of the magnetic field strength for the two initial magnetic field profiles. In this figure, we observe that the critical value α_c , depends strongly on the initial profile of the magnetic field. Actually, for the profile (II) we get $E_{GW,2}^{(B)}/(2M) = 3.267 \times 10^{-9}$, $C_{GW,2}/(2M) = 2.314 \times 10^{-8}$, and $\alpha_c = -7.08$. These difference suggest that the form of the magnetic field affects in a critical way the amount of the emitted gravitational waves and worths more elaborate study.

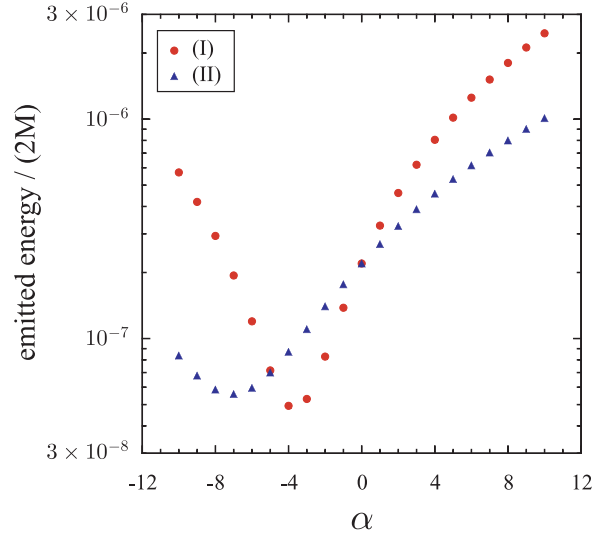


FIG. 12: Total energy emitted in quadrupole gravitational waves from the homogeneous dust collapse with two different initial magnetic field profiles as functions of the magnetic field strength. The filled circles correspond to results for the profile (I) and the filled triangles for profile (II)

VII. CONCLUSION

In this paper, we have studied the influence of magnetic fields on the efficiency of collapse in emitting gravitational waves. We have considered an interior Oppenheimer-Snyder solution describing collapsing dust and we studied how the amplitude and the waveform of the quadrupole axial perturbations were affected by the magnetic field, which actually enters as a second order perturbation term. These second order terms coming from the magnetic field are initially small but as the collapse proceeds they get amplified and become significant. For this study we have assumed that the magnetic field is axially symmetric and the $l_M = 1$ magnetic field perturbations are the ones that couple to the $l = 2$ axial perturbations of the gravitational field. Additional assumptions have been made concerning the initial data and the influence of the magnetic field in the exterior. That is, we assumed momentarily static initial data independent of the magnetic field and we have not taken into account the influence of the exterior magnetic field in the propagating gravitational waves.

The main result of this study is the proof of the strong influence of the magnetic field in the gravitational wave luminosity during the collapse. Depending on the initial profile of the magnetic field and its strength the energy outcome can be easily up to one order higher than what we get from the non-magnetized collapse. Additionally, we observed that the initial profile of the magnetic field perturbations can affect the energy output while it is possible to observe important phase shifts induced by the presence of the magnetic field. Since for a large initial radius the time needed for the black hole formation is longer, then the magnetic field acts for longer time on the collapsing fluid and its effect becomes more significant in the emitted gravitational wave signal.

Concluding, we believe that although this study might be considered as a "toy problem" it has most of the ingredients needed in emphasizing the importance of the magnetic fields in the study of the gravitational wave output during the collapse. It is obvious that 3D numerical MHD codes will provide the final answer to the questions raised here, but this work provides hints and raises issues that need to be studied.

Acknowledgments

We would like to thank Tomohiro Harada, Kenta Kiuchi, Hideki Maeda, and Kei-ichi Maeda for helpful conversations. This work was supported in part by the Marie Curie Incoming International Fellowships (MIF1-CT-2005-021979) and by the Grant-in-Aid for Scientific Research from the Ministry of Education, Culture, Sports and Technology of Japan (Young Scientist (B) 17740155). S.Y. is supported by the Grant-in-Aid for the 21st Century COE "Holistic Research and Education Center for Physics of Self-organization Systems" from the Ministry of Education, Culture, Sports, Science and Technology of Japan. KK acknowledges the support of the GSRT via the Pythagoras II program.

APPENDIX A: PERTURBED ENERGY-MOMENTUM TENSOR FOR THE ELECTROMAGNETIC FIELD INSIDE THE STAR

The non-zero components of the perturbed energy-momentum tensor $\delta T_{\mu\nu}^{(EM)}$ for the electromagnetic field associated with dipole ($l_M = 1$) perturbations inside the star are given by the following relations

$$\delta T_{\eta\eta}^{(EM)} = \frac{1}{24\pi} \left[\frac{2(b_1^2 + b_3^2)}{R^2 \sin^2 \chi} + \frac{b_2^2}{R^2 \sin^4 \chi} \right] P_0 - \frac{1}{12\pi} \left[\frac{b_1^2 + b_3^2}{R^2 \sin^2 \chi} - \frac{b_2^2}{R^2 \sin^4 \chi} \right] P_2, \quad (\text{A1})$$

$$\delta T_{\chi\chi}^{(EM)} = \frac{1}{24\pi} \left[\frac{2(b_1^2 + b_3^2)}{R^2 \sin^2 \chi} - \frac{b_2^2}{R^2 \sin^4 \chi} \right] P_0 - \frac{1}{12\pi} \left[\frac{b_1^2 + b_3^2}{R^2 \sin^2 \chi} + \frac{b_2^2}{R^2 \sin^4 \chi} \right] P_2, \quad (\text{A2})$$

$$\delta T_{\chi\theta}^{(EM)} = \frac{b_1 b_2}{12\pi R^2 \sin^2 \chi} (\partial_\theta P_2), \quad (\text{A3})$$

$$\delta T_{\chi\phi}^{(EM)} = -\frac{b_2 b_3}{12\pi R^2 \sin^2 \chi} \sin \theta (\partial_\theta P_2), \quad (\text{A4})$$

$$\delta T_{\theta\theta}^{(EM)} = \frac{b_2^2}{24\pi R^2 \sin^2 \chi} P_0 \gamma_{\theta\theta} + \frac{b_3^2 - b_1^2}{12\pi R^2} Z_{\theta\theta}^{l=2} + \frac{b_2^2}{12\pi R^2 \sin^2 \chi} P_2 \gamma_{\theta\theta}, \quad (\text{A5})$$

$$\delta T_{\theta\phi}^{(EM)} = \frac{b_1 b_3}{12\pi R^2} (S_{\theta:\phi} + S_{\phi:\theta})^{(l=2)}, \quad (\text{A6})$$

$$\delta T_{\phi\phi}^{(EM)} = \frac{b_2^2}{24\pi R^2 \sin^2 \chi} P_0 \gamma_{\phi\phi} + \frac{b_3^2 - b_1^2}{12\pi R^2} Z_{\phi\phi}^{l=2} + \frac{b_2^2}{12\pi R^2 \sin^2 \chi} P_2 \gamma_{\phi\phi}. \quad (\text{A7})$$

Following [29], we can expand the perturbed energy-momentum tensor for polar parity perturbations in terms of tensor spherical harmonics as

$$\Delta t_{\mu\nu} \equiv \begin{pmatrix} \Delta t_{AB} P_l & \Delta t_A^{\text{polar}} P_{l:a} \\ \Delta t_A^{\text{polar}} P_{l:a} & r^2 \Delta t^3 P_l \gamma_{ab} + \Delta t^2 Z_{ab}^l \end{pmatrix}, \quad (\text{A8})$$

where $Z_{ab}^l \equiv P_{l:ab} + l(l+1)P_l \gamma_{ab}/2$. [See, for the axial parity perturbations, equation (13).] Then, it has been found that the non-zero tensor-harmonic expansion coefficients of $\delta T_{\mu\nu}^{(EM)}$ for $l_M = 1$ are coupled with the $l = 0$ and $l = 2$ perturbations.

The expansion coefficients for the $l = 0$ perturbations are the following:

$$\Delta t_{\eta\eta} = \frac{1}{24\pi} \left[\frac{2(b_1^2 + b_3^2)}{R^2 \sin^2 \chi} + \frac{b_2^2}{R^2 \sin^4 \chi} \right], \quad (\text{A9})$$

$$\Delta t_{\chi\chi} = \frac{1}{24\pi} \left[\frac{2(b_1^2 + b_3^2)}{R^2 \sin^2 \chi} - \frac{b_2^2}{R^2 \sin^4 \chi} \right], \quad (\text{A10})$$

$$\Delta t^3 = \frac{b_2^2}{24\pi R^4 \sin^4 \chi}, \quad (\text{A11})$$

while the coefficients for the $l = 2$ perturbations are:

$$\Delta t_\chi^{(a)} = -\frac{b_2 b_3}{12\pi R^2 \sin^2 \chi}, \quad \Delta t = \frac{b_1 b_3}{12\pi R^2}, \quad (\text{A12})$$

$$\Delta t_{\eta\eta} = \frac{1}{12\pi} \left[\frac{b_2^2}{R^2 \sin^4 \chi} - \frac{b_1^2 + b_3^2}{R^2 \sin^2 \chi} \right], \quad \Delta t_{\chi\chi} = -\frac{1}{12\pi} \left[\frac{b_2^2}{R^2 \sin^4 \chi} + \frac{b_1^2 + b_3^2}{R^2 \sin^2 \chi} \right], \quad (\text{A13})$$

$$\Delta t_\chi^{(p)} = \frac{b_1 b_2}{12\pi R^2 \sin^2 \chi}, \quad \Delta t^2 = \frac{b_3^2 - b_1^2}{12\pi R^2}, \quad \Delta t^3 = \frac{b_2^2}{12\pi R^4 \sin^4 \chi}, \quad (\text{A14})$$

where (A12) belongs to axial parity perturbations, and (A13) and (A14) belong to polar parity perturbations.

APPENDIX B: PERTURBED ENERGY-MOMENTUM TENSOR FOR THE ELECTROMAGNETIC FIELD OUTSIDE THE STAR

The non-zero components of the perturbed energy-momentum tensor $\delta T_{\mu\nu}^{(EM)}$ for the electromagnetic field associated with dipole ($l_M = 1$) perturbations outside the star are given by the following relations

$$\begin{aligned} \delta \tilde{T}_{tt}^{(EM)} &= \frac{1}{24\pi} \left[f \left(\tilde{e}_2^2 + \frac{\tilde{b}_2^2}{r^4} \right) + \frac{2}{r^2} \left\{ \tilde{e}_1^2 + \tilde{e}_3^2 + f^2(\tilde{b}_1^2 + \tilde{b}_3^2) \right\} \right] P_0 \\ &\quad + \frac{1}{12\pi} \left[f \left(\tilde{e}_2^2 + \frac{\tilde{b}_2^2}{r^4} \right) - \frac{1}{r^2} \left\{ \tilde{e}_1^2 + \tilde{e}_3^2 + f^2(\tilde{b}_1^2 + \tilde{b}_3^2) \right\} \right] P_2, \end{aligned} \quad (B1)$$

$$\delta \tilde{T}_{tr}^{(EM)} = \frac{\tilde{e}_1 \tilde{b}_1 + \tilde{e}_3 \tilde{b}_3}{6\pi r^2} P_0 - \frac{\tilde{e}_1 \tilde{b}_1 + \tilde{e}_3 \tilde{b}_3}{6\pi r^2} P_2, \quad (B2)$$

$$\delta \tilde{T}_{t\theta}^{(EM)} = \frac{1}{12\pi} \left(-f \tilde{e}_2 \tilde{b}_3 + \frac{1}{r^2} \tilde{e}_1 \tilde{b}_2 \right) (\partial_\theta P_2), \quad (B3)$$

$$\delta \tilde{T}_{t\phi}^{(EM)} = -\frac{1}{12\pi} \left(f \tilde{e}_2 \tilde{b}_1 + \frac{1}{r^2} \tilde{e}_3 \tilde{b}_2 \right) \sin \theta (\partial_\theta P_2), \quad (B4)$$

$$\begin{aligned} \delta \tilde{T}_{rr}^{(EM)} &= \frac{1}{24\pi} \left[-\frac{1}{f} \left(\tilde{e}_2^2 + \frac{\tilde{b}_2^2}{r^4} \right) + \frac{2}{f^2 r^2} \left\{ \tilde{e}_1^2 + \tilde{e}_3^2 + f^2(\tilde{b}_1^2 + \tilde{b}_3^2) \right\} \right] P_0 \\ &\quad + \frac{1}{12\pi} \left[-\frac{1}{f} \left(\tilde{e}_2^2 + \frac{\tilde{b}_2^2}{r^4} \right) - \frac{1}{f^2 r^2} \left\{ \tilde{e}_1^2 + \tilde{e}_3^2 + f^2(\tilde{b}_1^2 + \tilde{b}_3^2) \right\} \right] P_2, \end{aligned} \quad (B5)$$

$$\delta \tilde{T}_{r\theta}^{(EM)} = \frac{1}{12\pi} \left(-\frac{1}{f} \tilde{e}_2 \tilde{e}_3 + \frac{1}{r^2} \tilde{b}_1 \tilde{b}_2 \right) (\partial_\theta P_2), \quad (B6)$$

$$\delta \tilde{T}_{r\phi}^{(EM)} = -\frac{1}{12\pi} \left(\frac{1}{f} \tilde{e}_1 \tilde{e}_2 + \frac{1}{r^2} \tilde{b}_2 \tilde{b}_3 \right) \sin \theta (\partial_\theta P_2), \quad (B7)$$

$$\delta \tilde{T}_{\theta\theta}^{(EM)} = \frac{r^2}{24\pi} \left(\tilde{e}_2^2 + \frac{\tilde{b}_2^2}{r^4} \right) P_0 \gamma_{\theta\theta} + \frac{1}{12\pi f} \left[\tilde{e}_1^2 - \tilde{e}_3^2 - f^2(\tilde{b}_1^2 - \tilde{b}_3^2) \right] Z_{\theta\theta}^{(l=2)} + \frac{r^2}{12\pi} \left(\tilde{e}_2^2 + \frac{\tilde{b}_2^2}{r^4} \right) P_2 \gamma_{\theta\theta}, \quad (B8)$$

$$\delta \tilde{T}_{\theta\phi}^{(EM)} = \frac{1}{12\pi} \left(-\frac{1}{f} \tilde{e}_1 \tilde{e}_3 + f \tilde{b}_1 \tilde{b}_3 \right) (S_{\theta:\phi} + S_{\phi:\theta})^{(l=2)}, \quad (B9)$$

$$\delta \tilde{T}_{\phi\phi}^{(EM)} = \frac{r^2}{24\pi} \left(\tilde{e}_2^2 + \frac{\tilde{b}_2^2}{r^4} \right) P_0 \gamma_{\phi\phi} + \frac{1}{12\pi f} \left[\tilde{e}_1^2 - \tilde{e}_3^2 - f^2(\tilde{b}_1^2 - \tilde{b}_3^2) \right] Z_{\phi\phi}^{(l=2)} + \frac{r^2}{12\pi} \left(\tilde{e}_2^2 + \frac{\tilde{b}_2^2}{r^4} \right) P_2 \gamma_{\phi\phi}. \quad (B10)$$

As for the interior, the non-zero expansion coefficients of $\delta T_{\mu\nu}^{(EM)}$ for $l_M = 1$ electromagnetic field perturbations are coupled with the $l = 0$ and $l = 2$ perturbations.

The expansion coefficients for the $l = 0$ perturbations are:

$$\Delta \tilde{t}_{tt} = \frac{1}{24\pi} \left[f \left(\tilde{e}_2^2 + \frac{\tilde{b}_2^2}{r^4} \right) + \frac{2}{r^2} \left\{ \tilde{e}_1^2 + \tilde{e}_3^2 + f^2(\tilde{b}_1^2 + \tilde{b}_3^2) \right\} \right], \quad (B11)$$

$$\Delta \tilde{t}_{tr} = \frac{\tilde{e}_1 \tilde{b}_1 + \tilde{e}_3 \tilde{b}_3}{6\pi r^2}, \quad (B12)$$

$$\Delta \tilde{t}_{rr} = \frac{1}{24\pi} \left[-\frac{1}{f} \left(\tilde{e}_2^2 + \frac{\tilde{b}_2^2}{r^4} \right) + \frac{2}{f^2 r^2} \left\{ \tilde{e}_1^2 + \tilde{e}_3^2 + f^2(\tilde{b}_1^2 + \tilde{b}_3^2) \right\} \right], \quad (B13)$$

$$\Delta \tilde{t}^3 = \frac{r^2}{24\pi} \left(\tilde{e}_2^2 + \frac{\tilde{b}_2^2}{r^4} \right), \quad (B14)$$

while the coefficients for the $l = 2$ polar parity perturbations have the form:

$$\Delta \tilde{t}_{tt} = \frac{1}{12\pi} \left[f \left(\tilde{e}_2^2 + \frac{\tilde{b}_2^2}{r^4} \right) - \frac{1}{r^2} \left\{ \tilde{e}_1^2 + \tilde{e}_3^2 + f^2 (\tilde{b}_1^2 + \tilde{b}_3^2) \right\} \right], \quad (\text{B15})$$

$$\Delta \tilde{t}_{tr} = -\frac{\tilde{e}_1 \tilde{b}_1 + \tilde{e}_3 \tilde{b}_3}{6\pi r^2}, \quad (\text{B16})$$

$$\Delta \tilde{t}_{rr} = \frac{1}{12\pi} \left[-\frac{1}{f} \left(\tilde{e}_2^2 + \frac{\tilde{b}_2^2}{r^4} \right) - \frac{1}{f^2 r^2} \left\{ \tilde{e}_1^2 + \tilde{e}_3^2 + f^2 (\tilde{b}_1^2 + \tilde{b}_3^2) \right\} \right], \quad (\text{B17})$$

$$\Delta \tilde{t}_t^{(p)} = \frac{1}{12\pi} \left(-f \tilde{e}_2 \tilde{b}_3 + \frac{1}{r^2} \tilde{e}_1 \tilde{b}_2 \right), \quad (\text{B18})$$

$$\Delta \tilde{t}_r^{(p)} = \frac{1}{12\pi} \left(-\frac{1}{f} \tilde{e}_2 \tilde{e}_3 + \frac{1}{r^2} \tilde{b}_1 \tilde{b}_2 \right), \quad (\text{B19})$$

$$\Delta \tilde{t}^2 = \frac{1}{12\pi f} \left[\tilde{e}_1^2 - \tilde{e}_3^2 - f^2 (\tilde{b}_1^2 - \tilde{b}_3^2) \right], \quad (\text{B20})$$

$$\Delta \tilde{t}^3 = \frac{1}{12\pi} \left(\tilde{e}_2^2 + \frac{\tilde{b}_2^2}{r^4} \right). \quad (\text{B21})$$

Finally, the coefficients for the $l = 2$ axial parity perturbations have the form:

$$\Delta \tilde{t}_t^{(a)} = -\frac{1}{12\pi} \left(f \tilde{e}_2 \tilde{b}_1 + \frac{1}{r^2} \tilde{e}_3 \tilde{b}_2 \right), \quad (\text{B22})$$

$$\Delta \tilde{t}_r^{(a)} = -\frac{1}{12\pi} \left(\frac{1}{f} \tilde{e}_1 \tilde{e}_2 + \frac{1}{r^2} \tilde{b}_2 \tilde{b}_3 \right), \quad (\text{B23})$$

$$\Delta \tilde{t} = -\frac{1}{12\pi} \left(\frac{1}{f} \tilde{e}_1 \tilde{e}_3 - f \tilde{b}_1 \tilde{b}_3 \right). \quad (\text{B24})$$

-
- [1] N. Andersson and K. D. Kokkotas, *Phys. Rev. Lett.* **77**, 4134 (1996); *Mon. Not. R. Astron. Soc.* **299**, 1059 (1998).
[2] O. Benhar, E. Berti, and V. Ferrari, *Mon. Not. R. Astron. Soc.* **310**, 797 (1999).
[3] N. Andersson and G. L. Comer, *Phys. Rev. Lett.* **87**, 241101 (2001).
[4] K. D. Kokkotas, T. A. Apostolatos, and N. Andersson, *Mon. Not. R. Astron. Soc.* **320**, 307 (2001).
[5] H. Sotani, K. Tominaga, and K. I. Maeda, *Phys. Rev. D* **65**, 024010 (2002).
[6] H. Sotani and T. Harada, *Phys. Rev. D* **68**, 024019 (2003); H. Sotani, K. Kohri, and T. Harada, *ibid* **69**, 084008 (2004).
[7] H. Sotani and K. D. Kokkotas, *Phys. Rev. D* **70**, 084026 (2004); **71**, 124038 (2005).
[8] B. C. Barish, in *Proceedings of the 17th International Conference on General Relativity and Gravitation*, edited by P. Florides, B. Nolan, and A. Ottewill (World Scientific, New Jersey, 2005), p. 24.
[9] <http://lisa.jpl.nasa.gov/>
[10] R. F. Stark and T. Piran, *Phys. Rev. Lett.* **55**, 891 (1985).
[11] T. W. Baumgarte and S.L. Shapiro, *Astrophys. J.* **526**, 941 (1999).
[12] M. Shibata, S. L. Shapiro, and K. Uryu, *Phys. Rev. D* **64**, 024004 (2001).
[13] M. Saijo, T.W. Baumgarte, S.L. Shapiro, and M. Shibata, *Astrophys. J.* **569**, 349 (2002).
[14] M. Shibata and S.L. Shapiro, *Astrophys. J. Lett.* **572**, L39 (2002).
[15] L. Baiotti, I. Hawke, P.J. Montero, F. Loffler, L. Rezzolla, N. Stergioulas, J.A. Font E. Seidel *Phys. Rev. D* **71**, 024035 (2005).
[16] T. W. Baumgarte and S. L. Shapiro, *Astrophys. J.* **585**, 930 (2003).
[17] M. D. Duez, Y. T. Liu, S. L. Shapiro, and B. C. Stephens, *Phys. Rev. D* **72**, 024028 (2005); **72**, 024029 (2005).
[18] M. D. Duez, Y. T. Liu, S. L. Shapiro, M. Shibata, and B. C. Stephens, *Phys. Rev. Lett.* **96**, 031101 (2006); *Phys. Rev. D* **73**, 104015 (2006).
[19] M. Obergaulinger, M. A. Aloy, and E. Müller, *Astron. Astrophys.* **450**, 1107 (2006).
[20] M. Obergaulinger, M. A. Aloy, H. Dimmelmeier, and E. Müller, *Astron. Astrophys.* **457**, 209 (2006).
[21] B. Giacomazzo and L. Rezzolla, preprint gr-qc/0701109.
[22] C. T. Cunningham, R. H. Price, and V. Moncrief, *Astrophys. J.* **224**, 643 (1978); **230**, 870 (1979); **236**, 674 (1980).
[23] E. Seidel and T. Moore, *Phys. Rev. D* **35**, 2287 (1987); E. Seidel, E. S. Myra, and T. Moore, *ibid* **38**, 2349 (1988); E. Seidel, *ibid* **42**, 1884 (1990).

- [24] H. Iguchi, K. Nakao, and T. Harada, Phys. Rev. D **57**, 7262 (1998); H. Iguchi, T. Harada, and K. Nakao, Prog. Theor. Phys. **101**, 1235 (1999); **103**, 53 (2000).
- [25] T. Harada, H. Iguchi, and M. Shibata, Phys. Rev. D **68**, 024002 (2003);
- [26] J. R. Oppenheimer and H. Snyder, Phys. Rev. **56** 455 (1939).
- [27] U. H. Gerlach and U. K. Sengupta, Phys. Rev. D **19**, 2268 (1979); **22**, 1300 (1980).
- [28] G. Lemaitre, Ann. Soc. Sci. Bruxelles A **53**, 51 (1933); R. C. Tolman, Proc. Natl. Acad. Sci. U.S.A. **20**, 169 (1934); H. Bondi, Mon. Not. R. Astron. Soc. **107**, 410 (1947).
- [29] C. Gundlach and J. M. Martín-García, Phys. Rev. D **61**, 084024 (2000); J. M. Martín-García and C. Gundlach, *ibid.* **64**, 024012 (2001).
- [30] P. M. Woods and C. Thompson, in *Compact Stellar X-Ray Sources*, edited by W. H. G. Lewin and M. van der Klis (Cambridge, Cambridge Univ. Press, 2005).
- [31] E. Nakar, A. Gal-Yam, T. Piran, and D. B. Fox, Astrophys. J. **640**, 849 (2006).
- [32] M. Shibata, M. D. Duez, Y. T. Liu, S. L. Shapiro, and B. C. Stephens, Phys. Rev. Lett. **96**, 031102 (2006).
- [33] P. Mészáros and M. J. Rees, Astrophys. J. Lett. **482**, L29 (1997); A. K. Sari, T. Piran, and J. P. Halpern, Astrophys. J. Lett. **519**, L17 (1999); T. Piran, Phys. Rep. **314**, 575 (1999).
- [34] S. L. Shapiro, Astrophys. J. **544**, 397 (2000); J. N. Cook, S. L. Shapiro, and B. C. Stephens, Astrophys. J. **599**, 1272 (2003); Y. T. Liu and S. L. Shapiro, Phys. Rev. D **69** 044009 (2004).
- [35] H. C. Spruit, Astron. Astrophys. **349**, 189 (1999).
- [36] M. Shibata, Y. T. Liu, S. L. Shapiro, and B. C. Stephens, Phys. Rev. D. **74**, 104026 (2006).
- [37] R. S. Hamadé and J. M. Stewart, Class. Quantum Grav. **13**, 497 (1996).
- [38] K. Kokkotas and B. Schmidt, Living Rev. Relativ. **2**, 4 (1992).
- [39] S. Chandrasekhar and S. Detweiler, Proc. R. Soc. London **A344**, 441 (1975).
- [40] R. H. Price, Phys. Rev. D **5**, 2419 (1972).